ASTRONOMY & ASTROPHYSICS
SUPPLEMENT SERIES

MAY 1989, PAGE 161

Astron. Astrophys. Suppl. Ser. **78,** 161-186 (1989)

Infrared spectroscopy of astrophysical ices: new insights in the photochemistry

R. J. A. Grim ([1]), J. M. Greenberg ([1]), M.S. de Groot ([1]), F. Baas ([1]), W. A. Schutte ([1,2]) and B. Schmitt([1,3])

([1]) Laboratory Astrophysics, Huygens Laboratory, University of Leiden, P.O. Box 9504, 2300 RA, Leiden, The Netherlands
([2]) NASA Ames Research Center, MS 245 – 6, Moffett Field, California 94035, U.S.A.
([3]) Laboratoire de Glaciologie et Géophysique de l'Environnement, 2 rue Molière, B.P. 96, F-38402 St. Martin d'Hères Cedex, France

Received September 5, 1988; *accepted January* 23, 1989

Summary. — Laboratory experiments simulating the photochemistry of icy grain mantles in molecular clouds are presented. The comparison of the infrared spectral features of photochemically and thermally evolved bimolecular mixtures, complex molecular mixtures, isotopically enriched mixtures, and matrix isolated mixtures leads to more definitive assignments. Ions as well as radicals and molecules are identified. The strong OCN^- and NH_4^+ absorption bands observed in the laboratory after photolysis and heating of $H_2O/NH_3/CO/O_2$ ice mixtures reproduce well the 4.62 and 6.86 μm interstellar absorptions seen towards W33A, indicating the likely presence of these ions in dust mantles. The detection of ions is an important step since it leads to a fuller understanding of the chemical reactions taking place in low temperature solids. The UV experiments demonstrate that NH_3 plays a critical role in the photochemistry leading to ion formation. The analysis of the IR spectra of the irradiated ices and argon mixtures, with or without NH_3 present, supports a chemical reaction scheme involving proton transfer reactions between NH_3 and acids that are photochemically produced. The ionic features in W33A indirectly indicate the initial presence of NH_3 in the dust mantles towards W33A. In addition to making line identifications, we also estimate the integrated infrared absorption band strengths of the ions involved, in order to be able to perform column density calculations which are important in astrophysical applications. Finally, the results presented here provide an extensive data base for future observations (with ISO) and specific suggestions are given.

Key words : chemical reactions — interstellar medium : dust — molecules — lines : identification.

1. Introduction.

In dense interstellar clouds it is generally accepted that an icy mantle is formed when condensable species collide with, and stick on, cold (± 10 K) dust particles (Greenberg, 1982b). One way to study these ice coatings is by looking for absorptions in the infrared spectrum since the mantle molecules will absorb the radiation emitted by embedded or infrared background sources at *definite* frequencies. Such IR sources can be a star forming region within the molecular cloud, a protostar, or a star that is situated behing an interstellar cloud, a background star. The specific absorptions seen in the IR spectra are related to the fundamental frequencies of oscillating molecules, and can be regarded as the *fingerprints* of these molecules (Allamandola, 1984). A summary of observations and identifications of some interstellar absorption bands in dense interstellar clouds is given in table I. Other reviews of observations in the mid-IR can be found elsewhere (e.g., Allamandola, 1984 ; Tielens and Allamandola, 1987).

Water ice appears to be responsible for the most widely observed solid state absorption : the 3.08 μm O—H stretching fundamental of frozen water has been observed towards numerous objects. The 6.0 μm bending fundamental has only been observed towards a few protostellar clouds (Willner *et al.*, 1982 ; Tielens and Allamandola, 1987) because of the difficulties intrinsic to ground based observations in this wavelength region which stems from atmospheric absorption. The peak position and shape of the 3.08 μm band appear to be sensitive tracers of the dust temperature (van de Bult *et al.*,1985). In the laboratory, on short time scales, crystallization of the ice structure takes place when the temperature is close to 130 K (Schmitt *et al.*, 1988a,b), resulting in a shift and narrowing of the absorption profile. Optical properties of H_2O have been extensively investigated as a function of temperature and ice composition (e.g., Hagen *et al.*, 1981, 1983a, 1983b ; Greenberg *et al.*, 1983 ; Kitta and Krätschmer, 1983 ; Léger *et al.*, 1983 ; Tielens *et al.*, 1983 ; Mukai and Krätschmer, 1986 ; and other references in these papers). For most interstellar objects the water-rich ice mantles are *amorphous,* as indicated by the shape of the 3.08 μm band, although recent observations also reported the presence of *annealed* and *crystalline* ice (van de Bult *et al.*, 1985 ; Geballe *et al.*, 1988 ; Greenberg

et al., 1988 ; Hodapp *et al.*, 1988 ; Rouan *et al.*, 1988 ; Smith *et al.*, 1988).

Carbon monoxide, CO, is the second most observed mantle component. It has been detected towards various objects and its IR spectral properties in molecular ices have recently been reviewed by Sandford *et al.* (1988). Because of its volatility, the suggestion has been made that it can also be used as a tracer of the dust temperature. A wide variation in CO column densities (relative to H_2O) has been deduced from CO observations (Grim and Greenberg, 1987a ; Schutte, 1988, hereafter S88; Sandford *et al.*, 1988). The precise interpretation of the CO observations is severely hampered by two *previously* unexpected phenomena, i.e., the ability of H_2O to trap CO up to crystallization temperatures (Bar-Nun *et al.*, 1985, 1987 ; Schmitt *et al.*, 1988a,b) and the temperature dependence of the CO infrared absorption coefficient in water ice (Schmitt *et al.*, 1988c).

Besides the temperature, the mantle compositions are, of course, also influenced by other local cloud conditions such as gas phase density, extinction, etc. In attempting to study the overall chemistry in a molecular cloud d'Hendecourt *et al.* (1985) have developed a time dependent model which takes into account both the chemistry leading to the formation of grain mantles by grain surface processes and ion-molecule gas phase chemistry.

In a second paper d'Hendecourt *et al.* (1986 ; hereafter dH86) empirically discussed the photochemical effects of the interstellar radiation field on the grain mante composition. The evidence for the existence of an internal UV radiation field in a molecular cloud is based on observational as well as theoretical considerations (Greenberg, 1971 ; Norman and Silk, 1980; Prasad and Tarafdar, 1983). In laboratory simulation studies it appeared that ultraviolet irradiation was capable of reproducing some of the observed interstellar features. For instance, Lacy *et al.* (1984) showed that the strong absorption at 2166 cm^{-1} in an irradiated $CO/NH_3 = 3/1$ mixture had a remarkable resemblance to the 4.62 μm absorption feature observed towards the highly obscured protostellar object W33A. A tentative identification with a C≡N stretch was given. Speculative assignments made later (Larson *et al.*, 1985 ; dH86) initially inspired us to perform this extensive study. Tielens *et al.* (1984) and dH86 discussed the formation of a feacture at 6.86 μm in irradiated astrophysical mixtures. Simple alcohols (e.g., methanol) and saturated hydrocarbons were added to the list of possible candidates for the 6.86 μm feature. Geballe *et al.* (1985) reported the appearance of a 4.9 μm (2041 cm^{-1}) feature in ices containing H_2S resembling the 4.9 μm absorption seen towards W33A. S88 particularly investigated the 3.3 – 3.4 μm C—H stretching features in the organic residues remaining after long time UV irradiation of astrophysically relevant ice mixtures (Greenberg, 1982a). For a more extended discussion of the observational evidence for photoprocessing inside molecular clouds, the reader is referred to S88.

As mentioned before, the *initial* incentive for this extensive study is the ongoing debate in the literature about the identification of some of the interstellar absorption features mentioned above. As is well known, identification of solid state absorption features is often not unique. A technique which may be applied in the laboratory to provide more unambigious identifications is *isotopic labelling* of the initial compounds (Pinchas and Laulicht, 1971). Isotope mass variations can affect the vibration frequency of a molecular bond. The IR transitions generally shift to a lower frequency with heavy isotope substitution. By measuring these shifts the structure of the band carrier involved can be defined. Applying this technique to our studies led to important information about the carriers that cause the absorption features.

Investigating the 2166 cm^{-1}(4.62 μm) absorption produced in CO/NH_3 mixtures as found by Lacy *et al.* (1984), we found that the induced ^{13}C and ^{15}N frequency shifts were characteristic of the OCN^- ion (Grim and Greenberg, 1987b). With this identification a new range of potential candidates for yet unidentified laboratory and interstellar absorptions became available. Following the OCN^- identification, our investigation of the CO/NH_3 experiment was then focussed on the identification of a band at 1457 cm^{-1} resembling the 6.86 μm feature seen towards various interstellar sources. The labelled CO/NH_3 experiments, however, *did not* supply sufficiently unique information. We therefore also varied the ice compositions to investigate under what conditions the 1457 cm^{-1} feature was preferentially produced. The presence of NH_3 appeared to be critical; irradiated NH_3/O_2 and NH_3/CO ices showed a strong 1457 cm^{-1} absorption, whereas in irradiated $CH_4/CO/N_2$, $H_2O/O_2/N_2$, H_2O/CO and H_2O/CH_4 ices it was absent. In section 3.1.1 (vi) its assignment to the ammonium ion (NH_4^+) will be discussed.

This paper presents the complete analysis of our experiments that led to the OCN^- and NH_4^+ assignments. After summarizing shortly the experimental procedures (Sect. 2), the results of the photochemistry of NH_3/O_2 ice mixtures (Sect. 3.1) are presented. This will be followed by a presentation of the results of the NH_3/CO ices (Sect. 3.2) and the astrophysically relevant ices (Sect. 3.3). For the last set of experiments compositions were chosen consistent with the observation that H_2O is the most abundant constituent in grain mantles (Greenberg, 1982b). We have not incorporated CH_4 or N_2 in the mixture since these molecules appeared not to be necessary for reproducing the strong interstellar absorption features and, secondly, they have been discussed elsewhere (dH86). In section 3.4 and 3.5, finally, we analyse the IR spectra after UV irradiation matrix isolated NH_3/O_2 or NH_3/CO mixtures. The matrix isolation experiments not only confirmed the identifications made, but also allowed us to obtain further information about the chemical reaction mechanisms.

In section 4 we discuss the reaction mechanisms leading to the observed components. The formation of ions

after UV irradiation of ammonia (NH_3) containing ices is explained in terms of *proton transfer reactions* in a solvent (here H_2O) when an acid interacts with ammonia. In chemistry, such phenomenon more generally is referred to as *"solvation"*. A brief review of the theoretical and experimental aspects of solvation is given in section 4.2. Its application to irradiated astrophysical ices is discussed in section 4.3. Calculations to derive the integrated IR band strength of NH_4^+ in ice are performed in section 4.4. Consequences for the interpretation of the IR features of in terstellar ice mantles are emphasized in section 5 where also the highlights of this paper are summarized. Astrophysical applications of these results can be found in Grim and Greenberg (1987b), Grim (1988) and Grim *et al.* 1989b.

A few remarks have still to be made. The formation of NH_4^+ and OCN^- in H_2O dominated grain mantles appears to depend strongly on the initial presence of NH_3, and somewhat less strongly on the presence of CO and O_2. Although CO has been widely observed, only a theoretical justification can be given for O_2 (d'Hendecourt *et al.*, 1985) since it has no observable IR transition. So far, solid NH_3 has not been *directly* detected in any interstellar object. The reasons for this are : i) the O—H stretch fundamental of H_2O at 3.08 μm overlaps with the N—H fundamental and is also 10 times stronger (d'Hendecourt and Allamandola, 1986), ii) the OH and NH bending modes near 6.0 μm also overlap, and iii) the NH_3 "umbrella" mode at 9.5 μm is totally obscured by the Si—O stretch absorption. Thus, *none* of the NH_3 fundamentals in interstellar IR spectra can be unambigiously detected. To attribute the 2.97 μm shoulder of the 3.08 μm absorption band as resulting from NH_3 is controversial, since crystalline ice can also account for this (Knacke *et al.*, 1982 ; Knacke and McCorkle, 1987 ; Geballe *et al.*, 1988 ; Smith *et al.*, 1988). One should be also extremely careful using the long wavelength wing of the water band (3.3 – 3.8 μm) as a measure for the NH_3 concentration since any base that forms a hydrogen bond with water will result in a lowering of the O—H fundamental frequency giving rise to a wing (Hagen *et al.*, 1983a). Furthermore, contribution from other X—H stretching compounds or from scattering large grains cannot be neglected. In any case, van de Bult *et al.* (1985) estimated that in the Taurus clouds the $[NH_3]/[H_2O]$ concentration is certainly less than 25%, and probably in the order of 10 – 15% (see also S88). In the laboratory it appeared that only 5% NH_3 ($H_2O/NH_3/O_2$ = 18/1/1) was required to produce a 1457 cm^{-1} absorption consistent with the obervational constraints.

2. Experimental methods.

The basics of our experimental set-up and analytical methods have been described earlier (Hagen *et al.*, 1979 ; Hagen, 1982). Up dated information can be found in S88 or Grim (1988). For the isotopically labelled experiments the following gases were used : $H^{18}O_2$ (99%), ND_3 (99.8%), $^{15}NH_3$ (99%), ^{13}CO (99%), $C^{18}O$ (99%), and $^{18}O_2$ (99.5%).

IR spectra from 4000 to 400 cm^{-1} (2.5 – 25 μm) were measured in reflection with a Michelson interferometer (Digilab FTS 15 B/D) after deposition, UV irradiation and heating. In order to obtain a good signal-to-noise spectrum in a short time, most spectra were taken with a 4 cm^{-1} resolution. This resolution did not affect the true absorption profiles since the IR bands were considerably *broadened* by the physical and chemical interactions in the *astrophysical solids*. Of course, this is not true for the argon experiments. The recorded IR spectra were plotted as the *absorbance* ($= {}^{10}\log(I/I_0)$) *versus* the *frequency* ν (cm^{-1}). Since, in most cases, we were not concerned with the absolute peak intensities, but merely with positions and shapes, arbitrary intensities given by autoscaling plotting routines, were used. When appropriate, scaling factors are noted. Finally, although many more or less equivalent definitions exist for the IR band strength per molecule, we shall consistently use the integrated cross section per molecule, A_x, as recommended by Person (1981) :

$$A_x = \frac{\int_{\nu_1}^{\nu_2} \tau_\nu \, d\nu}{N_x}$$

in which $\int_{\nu_1}^{\nu_2} \tau_\nu \, d\nu$ is the *integrated optical depth* of an absorption line ($\tau_\nu = \ln(I/I_0)$) and N_x is the number of absorbers per cm^{-2}. The dimension of A_x is cm $molecule^{-1}$. The absorption cross section per molecule (cm^2 $molecule^{-1}$) can be approximated by A_x/FWHM, where FWHM is the full-width- at-half-maximum. Suitable conversion tables to other units can be found in, e.g., Pugh and Rao (1976).

3. Results.

The interpretation of the results of photoprocessing of molecular ice mixtures is not always straigthforward. "*Standard*" matrix isolation spectroscopy generally leads to well resolved and sharp absorption lines unique for the *inert* matrix material used and appropriate assignments often can be made. In a molecular matrix environment, the absorption bands can shift significantly to lower, or higher, frequencies as a result of the interactions of the dopent with the *non-inert* host molecules. These interactions also lead to line broadening and, therefore, blending of absorption bands can occur. The resulting IR spectrum will become a superposition of many absorption bands. In order to calculate the isotope shifts, the peak positions have to be measured. Baseline correction procedures generally lead to inaccuracies in the peak positions which are a function of the depths and widths of the overlapping bands. We estimated the error in the observed frequencies of overlapping bands to be a few wavenumbers (< 5 cm^{-1}) and in a few cases somewhat larger (5 – 10 cm^{-1}).

With the identification of IR absorption bands as our ultimate goal, isotopic labelling was used to constrain the number of possible candidates for a particular absorption band. This technique is well explained in Pinchas and

Laulicht (1971) and Nakamoto (1986). Many references to matrix isolation studies, e.g. to the pioneer work of Milligan and Jacox (hereafter referred to as MJ or JM), can be found in the latter. When appropriate, other abbrevations will be denoted by [ ] after the given reference involved. In the following section, the experiments are described that led to the identification of the IR features.

3.1 UV IRRADIATION OF NH_3/O_2 ICES.

3.1.1 *Isotope substitution and line identifications.* — After preparation in the glass line the following mixtures were deposited : NH_3/O_2, $^{15}NH_3/O_2$, $NH_3/^{18}O_2$ and ND_3/O_2, all with a ratio of about 1/1. Subsequently, the mixtures were photolyzed and heated to room temperature in steps of 20 K. After each step, an IR spectrum was recorded. The IR spectra from 4000 – 500 cm^{-1} of the four mixtures are shown from top to bottom in figure 1. From left to right the spectra were taken after : deposition, 4 hr UV photolysis, heating to 120 K and 180 K. These temperatures were chosen because at 120 K all reactive and most of the volatile species (*not* NH_3, H_2O and some others) have disappeared, whereas at 180 K NH_3 had also sublimated. All spectra have been autoscaled and the number within each plot indicates the intensity scaling factor with respect to the spectrum taken as 100 after deposition. The 2000 – 1000 cm^{-1} IR spectra, where the OH/NH bending and N=O stretching vibrations are found, are plotted in figure 2.

A summary of the absorption frequencies in the labelled mixtures after deposition and photolysis at 12 K, and after heating to 180 K, is given in table II. The line assignments are based on a combination of the peak frequencies and isotope shifts with the emphasis on the latter since the isotope shifts are not as sensitive to variations in environments and conditions as are the peak positions. The experimental results and assignments are discussed as follows :

(i) *Ammonia* - NH_3

The IR spectrum of the deposited NH_3/O_2 mixture as shown in figure 1 (1st column, top) is similar to that of pure amorphous ammonia (Bertie and Morrison, 1980 ; d'Hendecourt and Allamandola 1986 [dHA86]). When heated to 120 K crystallization of NH_3 occured, as seen by a sharpening of the NH_3 IR bands (Fig. 1 and 2, 3rd column; Ferraro *et al.*, 1980 ; Sill *et al.*, 1980). Ammonia sublimated after heating above 120 K.

The IR spectrum of ND_3/O_2 after deposition (Fig.1, 1st column, bottom) shows numerous absorption bands which are assigned to NH_xD_y species (Reding and Hornig, 1951, 1955). Although the ND_3 had 99.8% purity, the IR spectrum indicates that a substantial fraction of the ND_3 was converted to hydrogenated NH_xD_y via hydrogen-deuterium exchange reactions taking place on the glass walls. These exchange reactions are difficult to eliminate since such polar species as NH_3 and H_2O easily stick on the walls and may re-appear during the experiment. As a result of the hydrogen-deuterium mixing, reliable assignments at 12 K are difficult to make. Above 180 K this problem is less severe, since most of the NH_xD_y will have sublimated.

(ii) *Nitrogen-oxygen radicals* - NO, NO_2, NO_3

Whereas NO was readily observed in the low temperature IR spectra by its 1875 cm^{-1} absorption line, NO_2 radical detection was impossible since its 1612 cm^{-1} absorption band (Becker and Pimentel, 1956 ; St. Louis and Crawford, 1965) is obscured by ammonia. In the visible region, however, NO_2 and NO_3 radicals were observed after plasma discharge depositions of samples containing both NH_3 and O_2 (van der Zwet, 1986).

(iii) *Nitrogen-oxygen molecules* - N_2O, N_2O_3, N_2O_4, N_2O_5

In contrast to the straigthforward assignments of the 1875 and 2236 cm^{-1} absorption lines to NO and N_2O, assignments to larger nitrogen-oxygen molecules were complicated by the numerous peak positions that have been reported in the literature for N_2O_3, N_2O_4 and N_2O_5 (see e.g., Fateley *et al.*, 1959 ; Morris *et al.*, 1987). The absorption lines at 959, 1302 and 1632 cm^{-1} were assigned to N_2O_3 on the basis of their observed isotope shifts (Tab. II). Similarly, the 752 cm^{-1} feature can be assigned to a bending mode of N_2O_4. The stretching modes of this molecule were not observed. Blending may be a reason for this. N_2O_5 is the only candidate that suits the 1701 cm^{-1} absorption. This molecule, formed by the recombination of an NO_2 and an NO_3 radical, has also been reportred in the IR spectra of the NH_3 and O_2 containing plasma discharges (van der Zwet, 1986).

The assignments to N_2O_3, N_2O_4 and N_2O_5 are further supported by the fact that their corresponding absorption bands did not disappear after heating to 180 K (this indicates that N_2O_3, N_2O_4 and N_2O_5 are at least as non-volatile as H_2O) and the fact that these compounds are liquids at 273 K and atmospheric pressure (Weast, 1983).

(iv) *The nitrite ion* - NO_2^-

The assignments of the 793, 820, 1233, 1337, 1385 and 1497 cm^{-1} absorption bands to NO_2^-, NO_3^-, NO_3^- and NH_4^+ (Tab.II) require some detailed comments, particularly since they involve the formation of ions by *non-ionizing* UV irradiation.

The NO_2^- ion has been studied in alkali halides (Narayanamurti *et al.*, 1966 [N66], Kato and Rolfe 1967 [KR67]), as well as in argon matrices doped with alkali metals and NO_2 (MJ69 ; Milligan *et al.*, 1970 ; MJ71). In spite of the disagreement in position and half width (FWHM) between our results and values reported for NO_2^- in the literature, which are due to the various environments, the ^{15}N and ^{18}O isotope frequency shifts are in excellent agreement (Tab. II). The measured FWHM ($\sim$ 25 cm^{-1}) of the NO_2^- ν_3 absorption line (1233 cm^{-1}) is consistent with a disordered structure (Brooker and Irish, 1971 [BI71]) rather than with a crystalline structure (KR67).

The ν_2 symmetric stretching vibration of NO_2^- absorbs

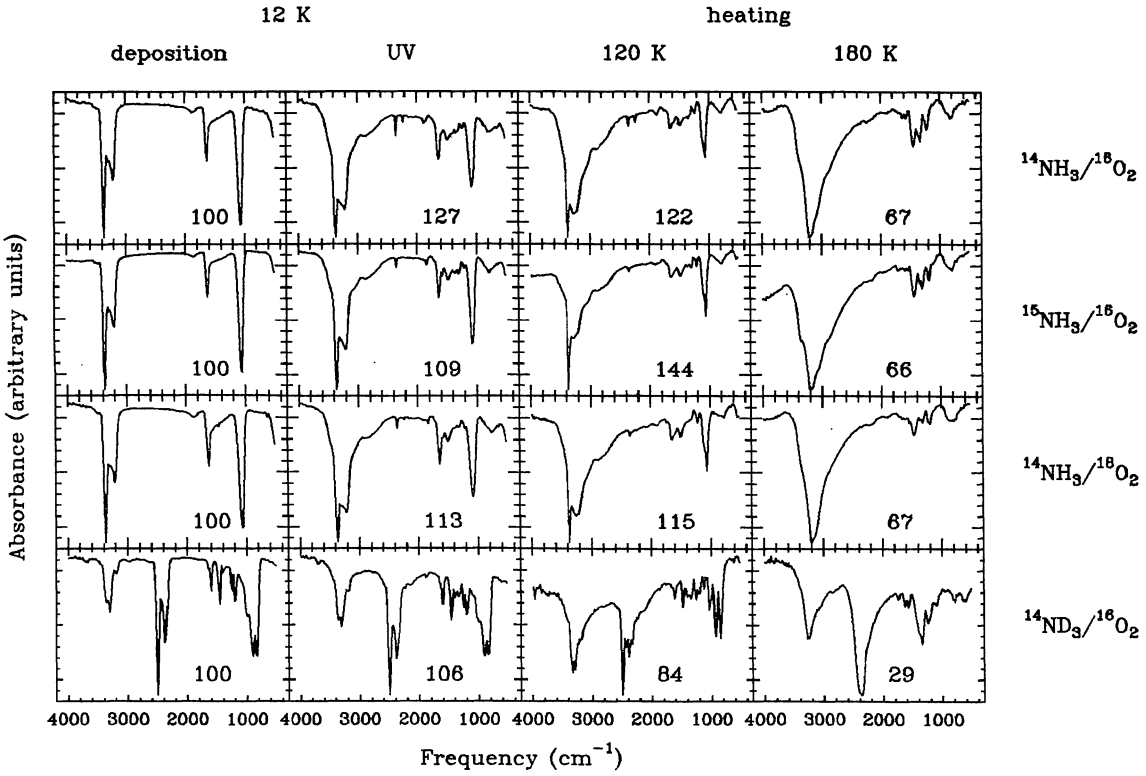

FIGURE 1. — IR spectra of labelled (^{15}N, ^{18}O, and D) $NH_3/O_2 = 1/1$ ices at different stages of their evolution. From left to right the spectra are shown after : a) deposition, b) UV irradiation for 2 hr., c) heating to 120 K, d) heating to 180 K. Since all spectra are autoscaled, the values shown in each spectrum denote the intensity scaling factors with respect to the reference spectra taken as 100 after deposition (left column). The spectra are plotted from 3900 to 500 cm^{-1}.

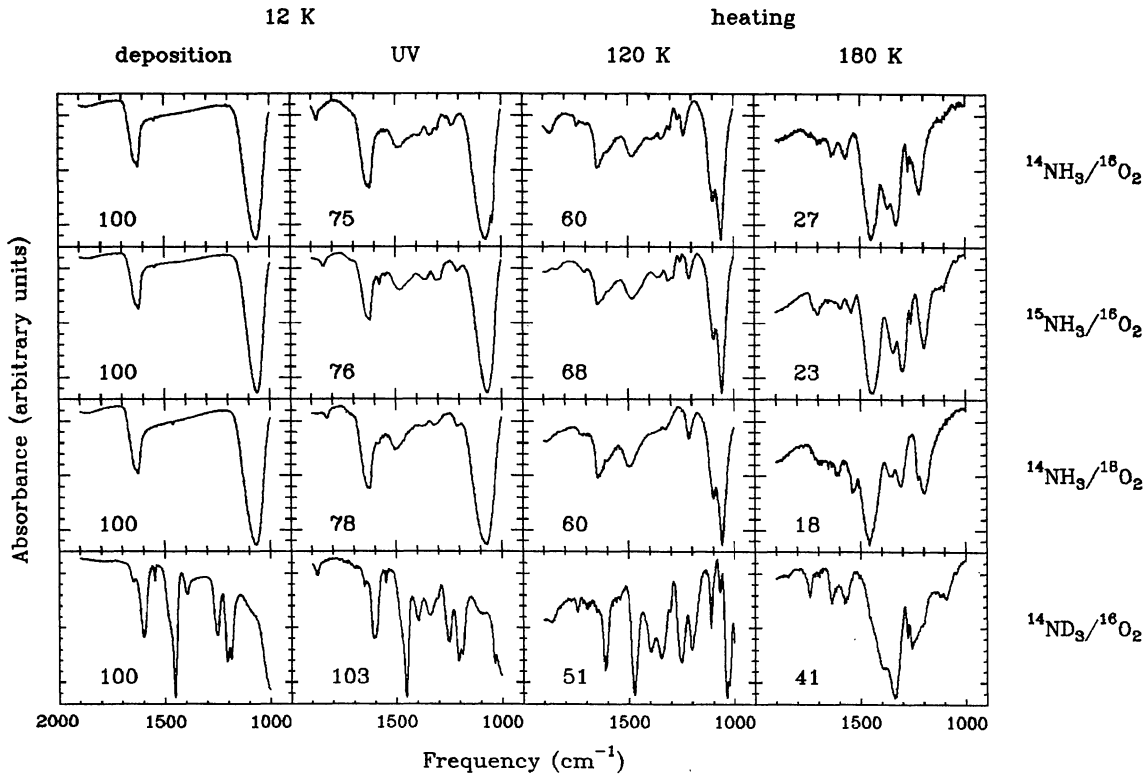

FIGURE 2. — Same as figure 1, but for the 1900 — 1000 cm^{-1} region.

at a slightly higher frequency, $\nu_2 - \nu_3 = 41$ cm^{-1}, in a KBr crystal (KR67), but is at least one order of magnitude weaker than ν_3 (BI71). This probably explains the absence of the ν_2 band in our IR spectra.

The assignment of the 798 cm^{-1} absorption line to the bending mode of NO_2^- is supported by the absolute frequency, but above all, by the observed isotope shifts (Tab. II).

(v) *The nitrate ion* - NO_3^-

The absorptions at 820, 1337 and 1385 cm^{-1} are assigned to NO_3^- on the basis of the observed isotope shifts in a KBr crystal (Tab. II). Although the peak positions do not agree with those measured in the KBr crystals (KR67), supporting evidence is found in solvation studies. There it was reported that, when $Tl^+NO_3^-$, $K^+NO_3^-$ and $Li^+NO_3^-$ were solvated in NH_3 or H_2O, the ν_3 mode of NO_3^- was split into two almost equally strong components (Ritzhaupt and Devlin, 1975 [RD75]; RD77a). The measured splittings were between 18 and 65 cm^{-1} (RD75 ; RD77a). When nitric acid (HNO_3) was solvated in ammonia or water the splittings were 20 and 65 cm^{-1}, respectively (RD77b). Irish and Davis (1968 [ID68]) observed a 48 cm^{-1} splitting when alkali metal nitrates were solvated in liquid water, being exactly the value we measured (Tab. II). Possibly this stems from the fact that our solid is as amorphous as liquid H_2O. It was concluded that the splitting and FWHM's are a sensitive probe for the interaction of the NO_3^- ion with neighbouring cations. For instance, a concentration dependent FWHM of the split ν_3 band of NO_3^- was reported by ID68 : when the nitrate molarity increased by a factor five the FWMH increased from 35 to 45 cm^{-1}. Although blending makes accurate measurements impossible, it is estimated that both 1337 and 1385 cm^{-1} absorptions have a FWHM of 35 cm^{-1} at 12 K. The increase of these widths to 49 and 47 cm^{-1}, respectively, at 180 K reflects an increased NO_3^- concentration. This is, of course, caused by the evaporation of the volatile components.

(vi) *The ammonium ion* - NH_4^+

Normally the deformation mode of NH_4^+ in alkali halides occurs between 1380 – 1420 cm^{-1} (Wagner and Hornig, 1950a, 1950b ; Ault *et al.*, 1975 and references therein), but it shifts to 1495 cm^{-1} when interacting $NH_4^+NO_3^-$ ion-pairs are formed by the solvation of HNO_3 with excess NH_3 in an argon matrix (RD77b). This position is in excellent agreement with the position observed in the NH_3/O_2 experiment (1497 cm^{-1}). Moreover, the assignment is consistent with the large frequency shift (measured at 180 K) upon deuterium substitution (Tab. II). Furthermore, the 1497 cm^{-1} band appeared only in samples *initially* containing NH_3. Also the FWHM's are reasonably consistent : the FWHM of the 1497 cm^{-1} feature is 70 cm^{-1} compared with the 50 cm^{-1} FWHM of the NH_4^+ deformation mode in the solvation study (see Fig. 2 in RD77b).

A study similar to that of RD77b has been performed by irradiating an NH_3/O_2 mixture in argon : at low temperature the acids HNO_2 and HNO_3 were stabilized in argon, but as soon the argon sublimated their spectral lines disappeared and NO_2^-, NO_3^- and NH_4^+ absorptions emerged. This study is described in section 3.4 and it not only supports the assignments made but it also provides information on the chemical reaction pathways.

3.1.2 *Temperature induced changes.* — After UV irradiation, the samples were heated in 20 K intervals. Column 3 and 4 of figures1 and 2 illustrate the changes in the IR when the temperature is 120 and 180 K, respectively. Initially, heating eliminated all radical species by recombination reactions, resulting in the formation of larger aggregates. The disappearance of the NO absorption feature at 1875 cm^{-1} is a clear example. Similarly, radicals like NH_2, HO_2 and OH were also expected, but their presence was not confirmed. Possible reasons for this can be that their absorptions were too weak to be observed, or that they immediately reacted with another nearby reactive species.

A second result of the heating was the crystallization of NH_3 just below 100 K (Ferraro *et al.*, 1980) and H_2O near 140 K (Hagen *et al.*, 1981). Since H_2O is only a minor component in the sample its crystallization did not affect the IR spectrum. Crystallization of NH_3 above 100 K was observed by sharpening of its spectral lines (Figs. 1 and 2 ; 3rd column).

Heating also led to the sublimation of volatile compounds. An example is the loss of N_2O between 140 and 160 K. Within a time scale of less than 1 hour, NH_3 sublimated above 160 K and H_2O above 180 K (monitored by the disappearance of the 750 cm^{-1} librational mode). After the evaporation of the volatiles, the remaining ions formed *"disordered"* salts (see below). Above 200 K no major changes were observed. A steady decrease in the absorption intensities of the remaining peaks merely indicates slow sublimation. When the sample was recooled to 12 K no spectral changes were observed indicating that they were irreversible.

During the entire heating process not only spectral lines disappeared, but some bands that were originally obscured emerged. The shape and position of the remaining absorption lines changed considerably. This is illustrated in figure 3 where we have plotted the central peak positions of the NH_4^+, NO_3^- (2x) and NO_2^- absorption bands *versus* the temperature. One recognizes the similarity of the temperature behavior of the different bands in the variously labelled mixtures. Note that in the deuterated experiment one of the NO_3^- absorption bands is obscured by the ν_4 vibration of NH_2D and therefore is not plotted (Fig. 2).

In the three non-deuterated samples, the NH_4^+ feature shifted approximately from 1497 cm^{-1} at 12 K to 1420 cm^{-1} for temperatures higher than 200 K. The two NO_3^- bands shifted only slightly when heated to 100 K, but at higher temperatures the splitting of the ν_3 mode of NO_3^- was gradually decreased until one band at 1350 cm^{-1} remained that blended with the 1420 cm^{-1} absorption of NH_4^+ (Fig.

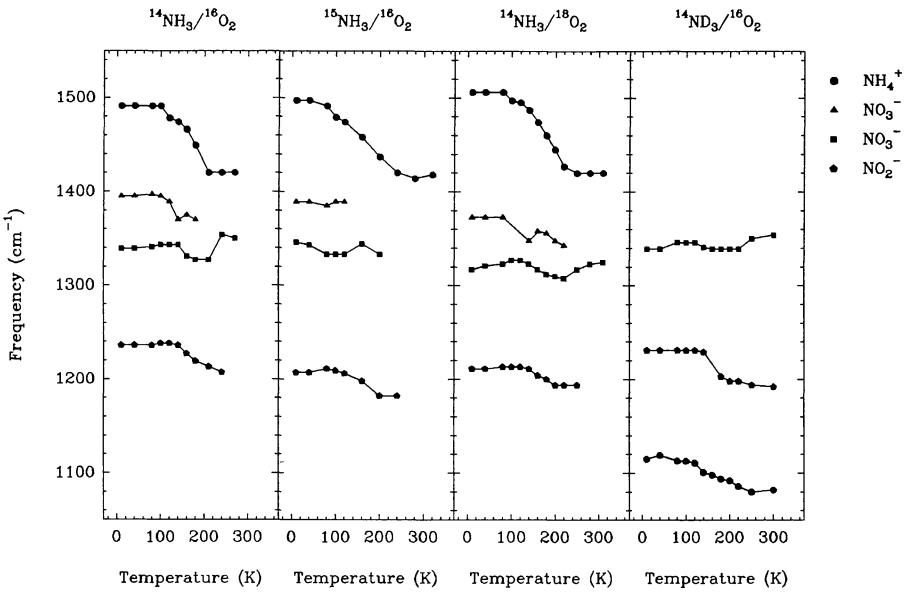

FIGURE 3. — Temperature dependence of the NH_4^+, NO_3^- (2x) and NO_2^- absorption lines. Note that in the ND_3/O_2 experiment one of the NO_3^- absorptions is obscured by NDH_2 (see Fig. 2).

4*a*). These features are characteristic of ammonium nitrate, NH_4NO_3 (Keller and Halford, 1949). In figure 4 we compare the IR spectrum of this compound (Fig. 4b) with the spectrum of a photolyzed $NH_3/N_2/O_2$ = 2/1/1 ice taken at 240 K (Fig. 4a). Although the match is not perfect we tentatively assign the observed IR spectrum to NH_4NO_3 on the basis of the reasonable agreement in the 1200 – 1500 and 2400 – 3400 cm^{-1} regions. Weaker NH_4NO_3 bands were not observed, but it seems likely that the NH_4NO_3 IR spectrum shown in figure 4b is saturated and therefore does not reflect the true relative line intensities.

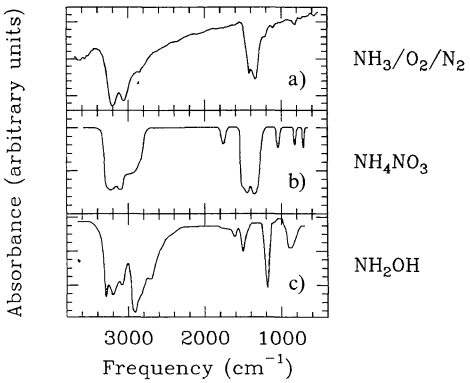

FIGURE 4. — a) The IR spectrum of irradiated $NH_3/O_2/N_2$ = 2/1/1 after heating to 240 K (top) compared with the spectra of b) crystalline NH_4NO_3 at 240 K (from Keller and Halford, 1949) and c) NH_2OH at 83 K (from Nightingale and Wagner, 1954). For this comparison the spectrum from the $NH_3/O_2/N_2$ = 2/1/1 was deliberately chosen for its best spectral resemblance with the NH_4NO_3 features. The spectrum of NH_2OH is given as an example of a compound that may contribute to the broad absorption observed below 3000 cm^{-1}.

The absorption excess to 2500 cm^{-1} (Fig.4a) might be explained by : (i) other N–H stretching components, e.g., from NH_2OH (Fig.4c), (ii) a significant part of N–H stretching components is hydrogen bonded resulting in a lowering of the N–H stretching frequency (Hagen *et al.*, 1983a), or (iii) scattering.

Taken together, at low temperature the ions are solvated, i.e., one observes the spectral IR features characteristic of single ions, whereas sublimation at a higher temperature leads to an increased ion fraction ; ion-contact pairs are formed and the IR spectrum is characteristic of salts. Because the sample is inhomogeneous in composition, a crystallization into a pure crystal cannot occur, merely the heating of all (salt-like) components leads to a *disordered crystalline-like structure.*

We close the discussion of NH_4NO_3 and its spectral features with a final consideration. As soon as the ammonium salts, NH_4X, vaporize the molecular species NH_3 and HX are formed by thermal decomposition (Chaiken *et al.*, 1962). In the case of NH_4NO_3 one expects to find NH_3 and HNO_3 in the gas phase. The sublimation and dissociation of the photolyzed materials could be probed with a mass spectrometer and should be a subject for further study.

3.2 UV IRRADIATION OF NH_3/CO ICES. — A detailed analysis of the UV irradiation of NH_3/CO ice mixtures was already given by Hagen (1982) who studied mixtures ranging in ratio from 1/3 to 1/100. Line assignments were reported and divided into three categories according to their degree of confidence. Based on a study of the growth curves and assignments, a reaction scheme was presented to account for the observed species. In this section we argue that some

of the assignments made by Hagen have to be revised in view of the new data presented here. Our data include the results found after UV irradiation of the following NH_3/CO ice mixtures: 10/1, 1/1 and 1/10. Isotope labelling studies with the 1/1 mixture were performed to gain extra information on specific band carriers.

3.2.1 *Isotope substitution and line identifications.* — IR spectra from 4000 to 500 cm^{-1} of the isotopically labelled NH_3/CO = 1/1 ice mixtures are shown in figure 5. From left to right are shown: the spectra after deposition, UV photolysis and heating to 120 and 180 K. The spectra taken after deposition show the IR features of NH_3 and CO isotopes. Note that the broad band centered at 2200 cm^{-1} is due to the coupling of the stretching mode with the librational modes of CO (Dubost 1976).

Ultraviolet irradiation gave rise to the appearance of new absorption bands (Fig.5, 2nd column) which are generally weaker than in the irradiated NH_3/O_2 ice mixtures. With heating, first CO evaporated (3rd column) and then, at a somewhat higher temperature, NH_3 also disappeared (4th column). Table III summarizes the peak frequencies observed after UV photolysis at 12 K and after heating to 180 K of the three differently labelled mixtures. Assignments and a comparison with the results found by Hagen (1982) are given in table IV. Agreed assignments are discussed first (i-iii), followed by a discussion of the disagreements (iv-v) and we end with the new assignments (vi-ix).

(i) *Radicals* - HCO, NH_2 *and* NH_2CO

During irradiation of the $^{14}NH_3/^{12}CO$ sample, two bands grew in at 1840 and 1854 cm^{-1}. Although the band positions are characteristic of a species containing the carbonyl (C=O) group, in the ^{13}C labelled experiment no corresponding bands were observed. This is probably the result of a somewhat lower initial ^{13}CO concentration. The temperature behavior, in particular the disappearance of both bands after heating to 40 K, indicates the reactive nature of their carriers. Although the fundamental frequency of HCO in a CO matrix is 1861 cm^{-1} (MJ64; Hagen 1982), the assignment of the 1854 cm^{-1} line to HCO is consistent with the position observed in irradiated molecular ices (1850 cm^{-1} : dH86 ; S88).

The NH_2CO assignment (1840 cm^{-1}) is taken from Hagen (1982). Attachment of the NH_2 group to the carbonyl group is believed to weaken the C=O bond, explaining the observed lowering in frequency compared to HCO. No reference spectra of NH_2CO are available. The NH_2 radical (1500 cm^{-1} : MJ65) has not been observed.

(ii) *Carbon dioxide* - CO_2

Because of its high IR band strength (Pugh and Rao, 1976 ; Sandford *et al.*, 1988) the 2344 cm^{-1} CO_2 absorption (Falk, 1987) is present in almost every UV photolysis experiment as a newly formed product (or as an impurity). During UV irradiation of NH_3/CO ice CO_2 is probably formed by reaction of CO with an oxygen atom or with an excited CO molecule (Hagen, 1982 ; Grim and d'Hendecourt, 1986).

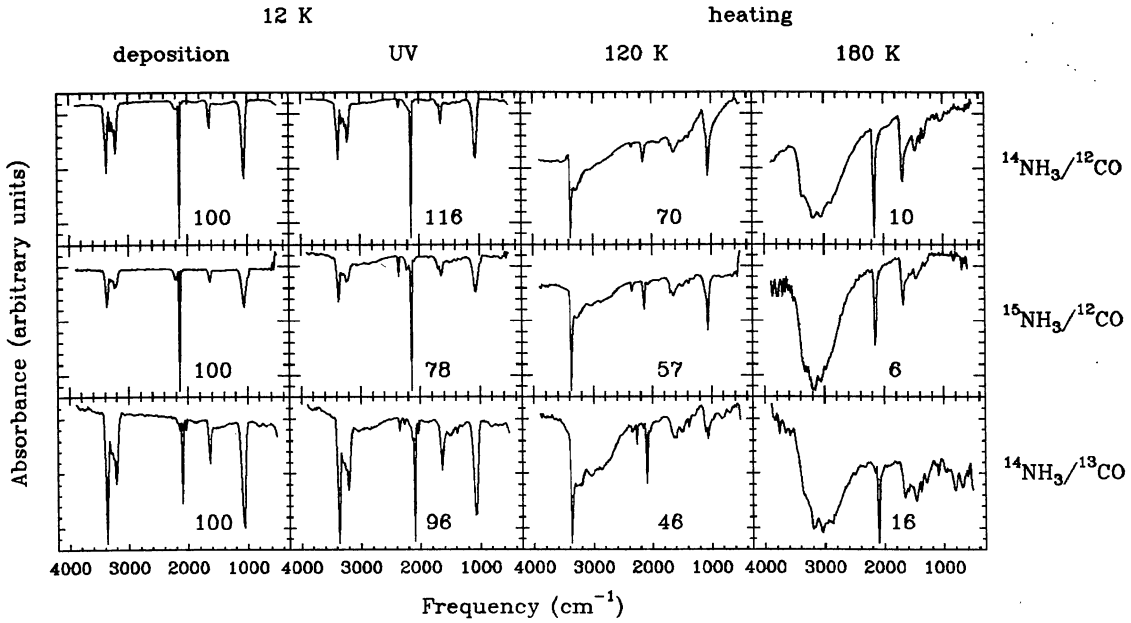

FIGURE 5. — IR spectra of labelled (^{13}C, ^{15}N) NH_3/CO ices at different stages of their evolution. From left to right the spectra are shown after: a) deposition, b) UV irradiation for 2 hr., c) heating to 120 K, d) heating to 180 K. Note that the NH_3/CO ratios after deposition are different by a factor three, probably as a result of saturation. Since all spectra are autoscaled, the values shown in each spectrum denote the intensity scaling factors with respect to the reference spectra taken as 100 after deposition (left column). The spectra are plotted from 3900 to 500 cm^{-1}.

(iii) *Formaldehyde* - H_2CO

For evidence of the presence of H_2CO one has to search for its two strongest absorptions at 1740 and 1500 cm^{-1}(Zhao 1988 : van der Zwet *et al.* 1988 and references therein). The relative sharpness of the latter feature should make it visible superimposed on the relative broad NH_4^+ absorption band, however, in the 1/1 experiment it has not been observed. Only in irradiated samples with excess CO (1/10 and 1/33) IR lines were assigned to H_2CO (Tab. IV).

(iv) *Formamide versus urea* - $HCONH_2$ *versus* NH_2CONH_2

Hagen (1982) assigned the 1388 cm^{-1} absorption to NH_4^+ (Tab. IV) on the basis of the good agreement with the NH_4^+ peak frequency in alkali halides. Absorption bands at 1497 and 1697 cm^{-1} were tentatively assigned to urea, NH_2CONH_2, and the bands located at 1266, 1715 and 1725 cm^{-1}were assigned to $HNONH_2$. In our experiments, the ^{13}C isotope shifts (in parenthesis) indicate the inclusion of carbon in the carrier of the 1323 (33), 1389 (6), 1609 (12) and 1684 (27) cm^{-1} absorption bands (Tab.III). The latter frequencies are typically for a C=O carbonyl stretch. Substitution of ^{15}N leads only to a shift of the 1323 cm^{-1} band (15 cm^{-1}).

In making appropriate assignments no literature data on isotope shifts was found. However, figure 6 clearly shows that urea (NH_2CONH_2) *cannot* account for the observed laboratory features. On the other hand, the figure shows that amorphous formamide ($HCONH_2$) is a better identification. Except for the width of the 1680 cm^{-1} band a good agreement between positions, intensities and widths is observed. Additionally, the spectral structure in the N–H stretching region (Fig. 7) seen at 2880 cm^{-1}(C–H stretch), 3200 and 3400 cm^{-1}(N–H stretches) were also reported for $HCONH_2$ (King, 1971). On the basis of these data we assign the 1323, 1389 and 1684 cm^{-1} features to

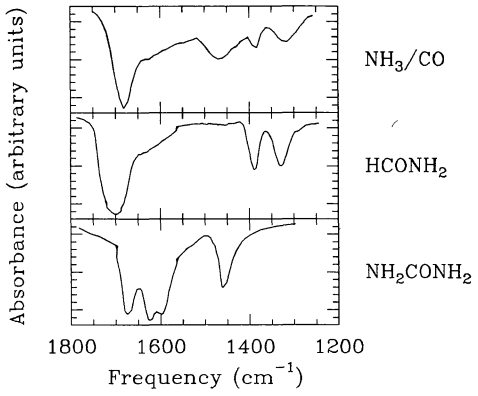

FIGURE 6. — The 1800 – 1200 cm^{-1} IR spectrum of irradiated NH_3/CO = 1/1 after heating to 180 K (top) compared with the spectra of $HCONH_2$ at 77 K (from King, 1971) and NH_2CONH_2 in a KCl pellet (from Stewart, 1957). Note that the broad band at 1470 cm^{-1} in the NH_3/CO spectrum is due to NH_4^+.Features outside this region are discussed in the text.

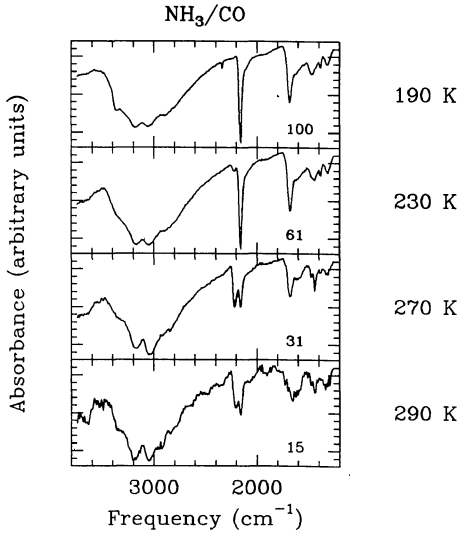

FIGURE 7. — The 3900 – 1300 cm^{-1} IR spectra of the irradiated and heated NH_3/CO = 1/1 mixture. From top to bottom the spectra were taken at T = 190, 230, 270 and 290 K, respectively. Note the appearance of the NH_4NCO absorption feature at 2214 cm^{-1} while the OCN^- absorption at 2155 cm^{-1} diminishes. $HCONH_2$ disappears above 270 K. The values in the spectra denote the scaling factors with respect to the spectrum as 100 taken at 190 K.

$HCONH_2$. The large discrepancies between matrix isolated $HCONH_2$(the basis for the assignments made by Hagen) and pure $HCONH_2$ (the basis for our assignments) are explained by hydrogen bond formation (King, 1971).

(v) *The ammonium ion versus urea* - NH_4^+ *versus* NH_2CONH_2

In a molecular ice, NH_4^+ does not absorb at 1388 cm^{-1} as reported previously (Hagen 1982), but at a 100 cm^{-1} higher frequency. The reasons for assigning the 1499 cm^{-1} absorption band to NH_4^+ are outlined in section 3.1.1.(vi). The tentative assignment made by Hagen (1982) to urea, NH_2CONH_2, *is not supported* by figure 6, although traces of urea can be detected in the spectra of heated samples (Sect. 3.2.2.).

(vi) *The cyanate ion* - OCN^-

The identification of the 2166 cm^{-1} absorption band towards the deeply embedded IR source W33A initiated this laboratory research project after it became clear that a strong band grew in near this position when irradiating (complex) mixtures containing CO and NH_3 (Hagen, 1982; Lacy *et al.*, 1984 ; dH86). From the possible candidates OCN^- appeared to satisfy best the laboratory constraints. For a further discussion of this band the reader is referred to Grim and Greenberg (1987b).

(vii) *The cyanide radical* - CN

A weak 2045 cm^{-1} absorption band is observed only in the $^{12}CO/^{14}NH_3$ experiment. The 2045 cm^{-1} carrier is

highly reactive as inferred from its temperature behavior. Two candidates were considered on the basis of their fundamental frequencies. The first candidate, the CO_3 radical, absorbs at 2053 cm^{-1} in a CO_2 matrix (Moll *et al.*, 1966 ; Weissberger *et al.*, 1967),but is rather unlikely since too little oxygen was available (this is also indicated by a weak CO_2 absorption band). The CN radical absorbs at 2046 cm^{-1} in an argon matrix (MJ67a) and seems to be a more reasonable candidate.

(viii) *Hydrogen cyanide and/or the cyanide ion* - HCN *and/or* CN^-

Two other bands at 2076 cm^{-1} (12 K) and 2100 cm^{-1} (180 K) are also characteristic of small C≡N stretching compounds (Chadwick and Edwards, 1973). At 12 K the 2100 cm^{-1} band was obscured by ^{13}CO absorption(2090 cm^{-1}) but became clearly visible after CO sublimation, while at the same time the 2076 cm^{-1} absorption disappeared.

The HCN molecule di ssolved in a CO matrix absorbs at 2104 cm^{-1} (King and Nixon, 1968) and gaseous HCN shows isotope shifts of about 35 cm^{-1} for ^{13}C and ^{15}N substitution (Chadwick and Edwards, 1973). For the cyanide ion the fundamental frequency is between 2060 and 2110 cm^{-1} in alkali halides (Seward and Narayanamurti, 1966) or near 2080 cm^{-1} in aqueous solution (Chadwick and Edwards, 1973). In matrix isolated NaCN and KCN the reported ^{13}C and ^{15}N shifts for CN^- are 31 and 42 cm^{-1}, respectively (Ismail *et al*, 1973). The labelling of the NH_3/CO mixtures does not provide a definitive basis for a distinction between HCN and CN^-.

(ix) *Carbonyl ions* - CO_2^-, HCO_2^- *and* $NH_2CO_2^-$

When searching for possible assignments for the 1609 cm^{-1} absorption feature the following ions were considered: CO_2^-, HCO_2^-, CO_3^{2-}, HCO_3^- and $NH_2CO_2^-$. The pros and cons of these compounds will be briefly summarized.

The argument that excluded the CO_3 radical, namely that too little oxygen was available, also applies to HCO_3^- and CO_3^{2-}. Furthermore, the reported isotope shifts of HCO_3^- (Bernitt *et al.*, 1965) are not in agreement with our results. The CO_2^- and HCO_2^- ions are better candidates since CO_2 was detected in minor quantities. The band position of CO_2^- is 1600 cm^{-1} in doped argon matrices (JM74 ; Kafafi *et al.*, 1984 [K84]) and 1671 cm^{-1} in KBr (Hartman and Hisatsune, 1966). In KBr, HCO_2^- absorbs at 1633 cm^{-1}(Hartman and Hisatsune, 1966). Although a comparison of the ^{13}C frequency shifts of these two components (JM74 ; Spinner and Rowe, 1979 ; K84) with our data cannot be made (we did not observe the band in the ^{13}C labelled NH_3/CO experiment), we tentatively assign the 1609 cm^{-1} band to HCO_2^- for reasons outlined in section 3.3.1(vii).

Ammonium carbamate, $NH_2CO_2NH_4$, can be formed by condensation of gaseous mixtures of NH_3 and CO_2. The resulting IR spectrum was interpreted in terms of NH_4^+ and $NH_2CO_2^-$ ions (Frasco, 1964). The NH_4^+ ion in ammonium carbamate absorbs at a higher frequency than NH_4^+ in alkali halides ; 1460 and 1483 cm^{-1} *versus* 1400 cm^{-1}, respectively. The carbamate ion, $NH_2CO_2^-$, shows strong bands at 1115 cm^{-1}(symmetric CO_2 stretch), 1404 cm^{-1}(C–N stretch) and 1525 cm^{-1}(asymmetric CO_2 stretch) and a very broad one from 2500 to 3500 cm^{-1} (N–H stretches). The weak 1132 and 1553 cm^{-1} absorption bands in the NH_3/CO experiment might result from $NH_2CO_2^-$, but are not supported by the isotope shifts.

(x) *Other features*

The assignment of the absorption feature at 2214 cm^{-1} to NH_4NCO will be discussed in section 3.2.2. Absorption in the NH_3/CO = 1/10 samples are assigned in agreement with the work of Hagen (Tab.IV). For example, the 2263 cm^{-1} absorption band is ascribed to HNCO (JM64; MJ65), while the absence of HNCO in the 10/1 and 1/1 experiments is explained in section 4. Furthermore, bands are assigned to NCO and NCCO (MJ67b), HOCN (JM64), C_3O_2 (Jacox *et al.*, 1965 ; deKock and Weltner, 1971). The latter assignment is based on irradiation experiments of solid non-diluted CO (unpublished results). The 2028 cm^{-1}absorption band in the 1/10 experiment is somewhat mysterious. HNC could be a good candidate (MJ67a), but an assignment to C_3 (deKock and Weltner, 1971) is also possible. Finally, the bands observed near 1300 cm^{-1} may be assigned to N_2H_2 (Rosengren and Pimentel, 1965), whereas N_2H_4 could be a possible identification for the 1090 cm^{-1} absorption observed at 180 K (Catalano *et al.*, 1963 ; Roux and Wood, 1983).

3.2.2 *Temperature induced changes.* — The IR spectra after heating to 120 and 180 K are shown in the last two columns of figure 5. As already described for the NH_3/O_2 mixtures, heating led to the disappearance of reactive and volatile species. What remained after heating to 180 K is a rather non-volatile sample, when compared to H_2O, that shows the characteristics of N—H stretching and C=O stretching compounds as deduced from their corresponding absorptions from 3600 to 2500 cm^{-1} and from 1800 to 1200 cm^{-1}, respectively.

When the sample was heated beyond 180 K a slow and steady decrease of all bands by sublimation was observed, although the OCN^- absorption band decreased faster than others. With the OCN^- disappearance a new feature grew in at 2214 cm^{-1} (Fig. 7). In a photolysis study of gaseous NH_3 and CO it was found that ammonium cyanate, NH_4NCO, was the major photolysis product as identified by it 2220 cm^{-1} absorption band (Hubbard *et al.*, 1975).Consequently we assign the 2214 cm^{-1} absorption to NH_4NCO. It is noteworthy that Hubbard *et al.* also reported the thermal conversion of ammonium cyanate into urea, NH_2CONH_4. In fact, some evidence for traces of urea is seen in figure 8.

Prolonged heating overnight at 290 K finally led to a disappearance of all spectral features, but on the aluminum block a residue remained. These residues were non-volatile at room temperature and have been subject of an

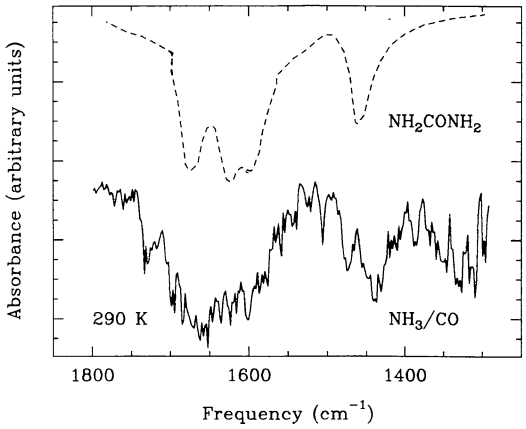

FIGURE 8. — The IR spectra in the 1800 – 1300 cm^{-1} region of irradiated NH_3/CO = 1/1 at T = 290 K compared with urea, NH_2CONH_2 (from Stewart, 1957).

extensive study in relation to the IR observations towards the Galactic Center (S88). In S88 the residues (after long irradiation/condensation times) were first analyzed in the infrared and later on with gas and high pressure liquid chromatography (GC and HPLC) in combination with mass spectrometry (MS : Agarwal *et al.*, 1985 ; S88). The molecules identified in the GC/MS study are closely related to the molecules identified in the IR studies (Tab. V).

3.3 UV IRRADIATION OF $H_2O/NH_3/CO/CO_2$ ICES. — Here the results of the UV irradiation of *astrophysically relevant* ice mixtures are discussed. Initially, an ice with composition $H_2O/NH_3/CO/O_2$ = 10/1/1/1 was chosen, but additionally we also varied the H_2O and O_2 concentrations by a factor four. Variation of the H_2O concentration had little effect on the ultimate molecular composition of the irradiated samples. On the other hand, the intensities of some bands could be influenced by the variation of the O_2 concentration.

The followed experimental procedures differed slightly from the standard ones. Namely, condensation and irradiation were *simultaneous*. The main reason for this was to obtain higher photolysis yields, since an accreting ice layer, mostly composed of H_2O, rapidly becomes optically thick for UV with increasing thickness. Since thin condensation layers give weak IR signals, the simultaneous condensation and irradiation procedure provides the required photolysis efficiency and minimum column densities for detection. As a matter of fact, such an experiment better simulates the actual interstellar processes. The disadvantage of this method lies in the fact that no estimates for IR band strengths can be made since the reference spectrum after condensation is not recorded. Typically, the samples were grown and irradiated for one or two hours with an estimated condensation rate that is an order of magnitude less than the one used in the experiments described earlier (Sect. 3.1 and 3.2). The next step was to heat the samples to 35, 60, 100, 120, 140, 160 and 176 K, respectively. To study the effects of slow annealing the samples were annealed at 176, 196 and 214 K for times of 20h00m, 3h30m and 1h30m, respectively. We compare our results, where appropriate, with the work of dH86 ($H_2O/CO/CH_4/NH_3$ = 6/2/1/1), and S88 ($H_2O/CO/NH_3$ = 5/2/1 and H_2O/CO = 3/1).

3.3.1 *Isotope substitution and line identifications.* — Figure 9 compares the 4000 – 500 cm^{-1} IR region of $H_2O/NH_3/CO/O_2$ = 10/1/1/1 taken after simultaneous deposition and UV irradiation at 12 K with that of condensed and *subsequently* irradiated NH_3/O_2, NH_3/CO and NH_3/H_2O = 1/1. In figure 10 a similar comparison is shown for the 2000 – 1000 cm^{-1} region of a 10/1/1/0.25 sample with irradiated NH_3/O_2, NH_3/CO ices. Also a comparison with the 10/1/1/1 mixture is given. The effects of isotopic labelling of the 10/1/1/0.25 mixture are

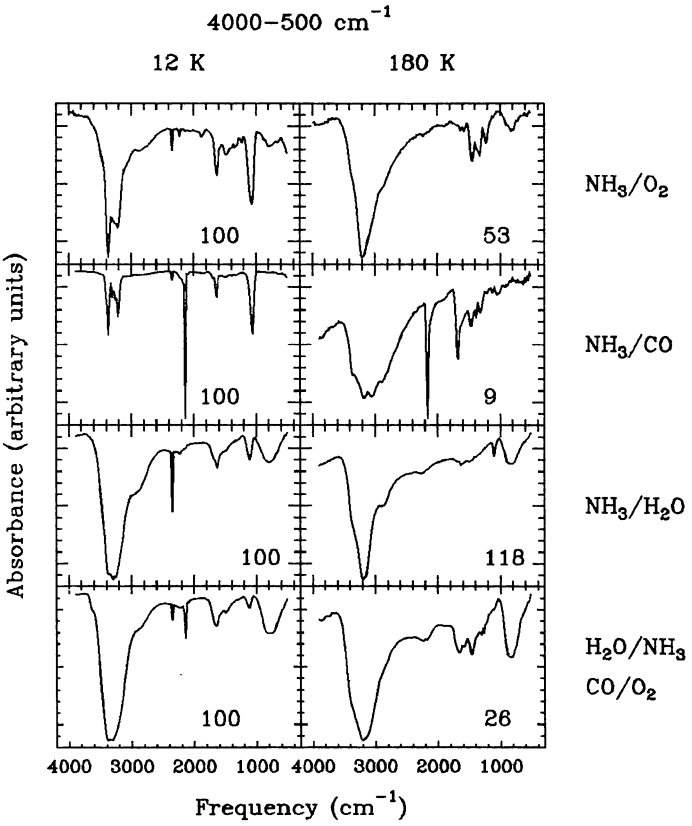

FIGURE 9. — IR spectra of $H_2O/NH_3/CO/O_2$ = 10/1/1/1 (bottom) after simultaneous deposition and irradiation at 12 K (left) and after heating to 180 K (right). For comparison the IR spectra of NH_3/O_2, NH_3/CO and NH_3/H_2O (= 1/1) are also shown. These spectra were taken after irradiation of the condensed samples at 12 K and after heating to approximately 180 K. Only the NH_3/H_2O spectrum is taken at slightly lower temperature (~ 170 K). Since all spectra are autoscaled, the values shown in each spectrum denote the intensity scaling factors with respect to the reference spectra taken as 100 after deposition (left column). The spectra are plotted from 3900 to 500 cm^{-1}.

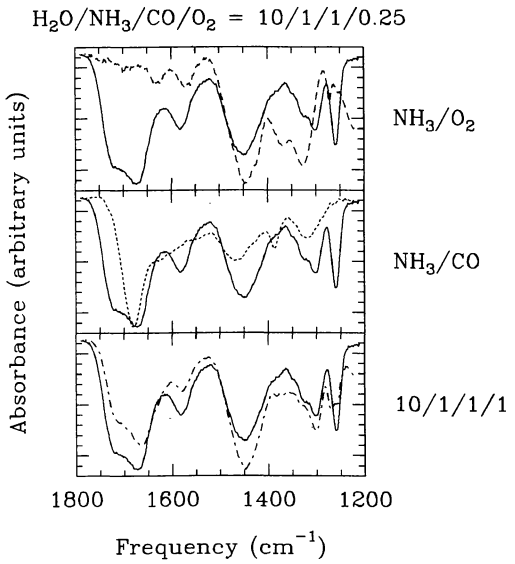

FIGURE 10. — The 1800 – 1200 cm^{-1} region of $H_2O/NH_3/CO/O_2 = 10/1/1/0.25$ compared with NH_3/O_2, NH_3/CO (= 1/1) and the 10/1/1/1 mixture. All spectra are taken at about 180 K. Note the following facts : (i) the NH_4^+ band near 1450 cm^{-1} is observed in all sepctra ; (ii) the IR bands between 1500 and 1800 cm^{-1} are from carbonyl groups (see also text and Fig. 11) ; and (iii) the oxygen concentration influences the relative intensities of IR bands.

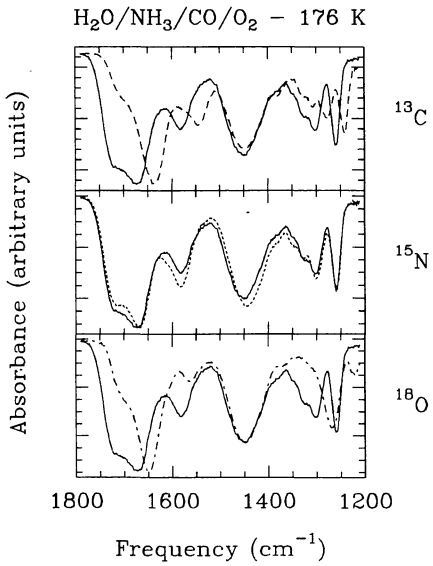

FIGURE 11. — Isotopic labelling of $H_2O/NH_3/CO/O_2 = 10/1/1/0.25$ with ^{13}C, ^{15}N and ^{18}O isotopes. All IR spectra were taken after 20h annealing at 176 K. The carbon and oxygen isotope shifts indicate the inclusion of these atoms in the carriers of several IR bands.

portrayed in figure 11. Except for the band at 1500 cm^{-1}, all IR lines shift with ^{13}C and ^{18}O substitution indicating the likely presence of carbonyl (C=O) groups. Line assignments were made with the help of the isotopically labelled ices and the results of section 3.1 and 3.2. Table VI summarizes (i) the band positions at various temperatures, (ii) the isotope shifts, (iii) the temperature range in which the absorptions are observed, and (iv) the assignments made. The following discussion elucidates the assignments.

(i) *Radicals* - NO *and* HCO

Although NO absorption is observed, no trace of HCO could be detected. dH86 and S88 report both absorptions in their experiments. A possible explanation for the absence of HCO is the lower CO concentration in our experiments (<10% compared with ~ 33% in dH86 and S88).

(ii) *Carbon dioxide* - CO_2

Both the $^{12}CO_2$ and $^{13}CO_2$ absorption , 2344 and 2276 cm^{-1}, respectively, are identified in all CO and O_2 containing astrophysical mixtures. The relative weakness of the CO_2 absorptions compared with the results of dH86 and S88 is attributed to the lower initial CO concentration in our experiments.

(iii) *Nitrogen-oxygen compounds* - NO_2^-

Examination of figure 10 and 11 suggests that in the astrophysical mixture little nitrogen-oxygen compounds are formed. Except for the 1454 cm^{-1} absorption (position at 176 K), the carriers of the other strong bands in the 2000 – 1000 cm^{-1} region contain carbon and oxygen as evidenced by the isotope shifts. Only a weak absorption, observed after heating to 196 K, is assigned to NO_2^- (1231 cm^{-1}). The weakness of the NO_2^- line and the absence of NO_3^- absorption lines indicate that in the photochemistry of astrophysical ices molecular oxygen does not play a crucial role as long as its initial concentration is <10% .

N_2O (2234 cm^{-1}) was observed by S88, but was concluded to be an air contamination. Also dH86 identified N_2O. We have not observed the N_2O absorption line. Similarly, no evidence for the presence of N_2O_3, N_2O_4 or N_2O_5 has been found.

(iv) *The ammonium ion* - NH_4^+

The only feature appearing in all irradiated ices is the NH_4^+ absorption shortwards of 1500 cm^{-1} (Fig. 9). In the H_2O/NH_3 experiment this feature is visible in the low frequency shoulder of the H_2O/NH_3 absorption band. Arguments for the NH_4^+ assignment have been outlined in section 3.1.1 (vi).

(v) *The cyanate ion* - OCN^-

The optical depth of the OCN^- absorption at 2166 cm^{-1} is less than 10% of the NH_4^+ optical depth. In experiments with a higher CO concentration (dH86 ; S88 ; or $H_2O/NH_3/CO$ = 4/2/1) the optical depth of OCN^- can exceed that of NH_4^+. This is evidently a concentration effect. A higher CO or a lower H_2O or O_2 concentration increases the strength of the OCN^- band over that of NH_4^+. Formation of NH_4NCO was not observed, probably because its column density is too low. The weak OCN^- band could account for this.

(vi) *Formamide* - $HCONH_2$

In earlier publications (e.g., Allamandola, 1984 ; dH86) it was reported that the simultaneous disappearance of the 2166 and 1690 cm^{-1} absorptions bands with warm up implied an identification of both lines with one molecule. This led to the speculation that pyruvo (iso) nitrile, CH_3COCN, could be a reasonable identification for both bands (dH86). However, in our results the optical depths of these bands *were not correlated.* In analogy with the NH_3/CO experiments, we assign the 1670 cm^{-1} absorption line to $HCONH_2$. Although difficult to observe due to blending, its weaker absorption lines at 1329 and 1389 cm^{-1} are seen as shoulders on the 1300 and 1454 cm^{-1} absorption bands, respectively (Fig. 10).

(vii) *The formate ion* - $HCOO^-$

An absorption band at 1580 cm^{-1} became visible as a shoulder on the blended H_2O/NH_3 absorption band after the temperature was raised to 98 K. Heating to 176 K was required to observe the band as a local minimum (Fig. 9). This band was also observed by dH86 and S88, but no assignments were given.

It appeared that the 1580 cm^{-1} absorption was only visible in samples containing CO, H_2O *and* NH_3. For example, it was absent in the IR spectra of irradiated $H_2O/NH_3/O_2$, H_2O/NH_3 or H_2O/CO ices. An absorption at 1570 cm^{-1} was observed in an irradiated NH_3/O_2 ice, but heating above 200 K it shifted to a lower frequency (1553 cm^{-1}). On the other hand, the 1580 cm^{-1} line in the $H_2O/NH_3/CO(/O_2)$ ices shifted in the opposite direction (1612 cm^{-1}) eliminating the possibility that both absorptions arise from the same carrier. Furthermore, labelling with ^{13}C and ^{18}O isotopes (Fig.11, Tab. VI) clearly demonstrated the presence of both carbon and oxygen in the carrier of the 1580 cm^{-1} absorption feature. More specifically, the shifts are characteristic of carboxylic acids (PL71).

The simplest carboxylic acid is formic acid, HCOOH, and is preferentially made in H_2O/CO ices exposed to UV irradiation (S88). Figure 12 shows that HCOOH cannot account for the 1580 cm^{-1} band, but an assignment to the formate ion, $HCOO^-$, is supported by the following arguments : (i) in an aqueous solution of potassium formate, $HCOO^-$ absorbs at 1585 cm^{-1} whereas its fundamental frequency in salts varies between 1567 and 1620 cm^{-1} (Ito and Bernstein, 1956 [IB56]) ; (ii) the ^{13}C and ^{18}O isotope shifts (Tab. VI) are in agreement with the literature values of $\sim$ 37 cm^{-1} for ^{13}C (PL71 ; Spinner and Rowe, 1979 [SR79]) and $\sim$ 13 cm^{-1} for ^{18}O (PL71) ; (iii) the estimated FWHM of the 1580 cm^{-1} band in the $H_2O/NH_3/CO/O_2$ experiment is 40 cm^{-1} and compares reasonably with the FWHM of $HCOO^-$ in aqueous solution of 50 cm^{-1} (IB56 ; Hammaker and Walters, 1964 [HM64]) ; (iv) the formation of $HCOO^-$ is expected after interaction of NH_3 with HCOOH (Sect. 4).

The other bands (1263 and 1304 cm^{-1}) are assigned to $HCOO^-$ on basis of the reported ^{13}C and ^{18}O shifts for the formate ion in sodium formate (22 and 39 cm^{-1}, respectively : HW64 ; SR79). The absorption at 887 cm^{-1} showed isotope shifts characteristic for the OCO scissoring mode of $HCOO^-$ (HW64 ; PL71 ; SR79).

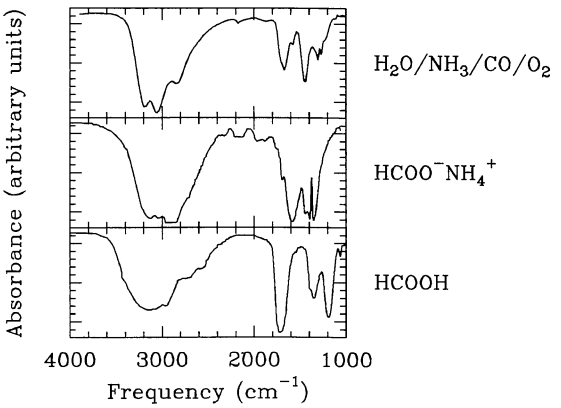

FIGURE 12. — The IR spectra of formic acid, HCOOH, and ammonium formate, $HCOO^-NH_4^+$ (Pouchert, 1981) compared with the IR spectrum of irradiated $H_2O/NH_3/CO/O_2$ = 10/1/1/1 taken after heating to 176 K for 20h.

The assignment of any of the last three bands to CO_2^{2-}, instead of $HCOO^-$, is not totally exluded since CO_2^{2-} shows similar isotope shifts as $HCOO^-$ (Kafafi *et al.*, 1984). However, the isotope shifts reported for the carbonyl stretch of the CO_2^{2-} ion are larger than the ones observed for the 1580 cm^{-1} band, thus favoring the $HCOO^-$ assignment rather than a CO_2^{2-} assignment.

(viii) *The carbonate ion* - CO_3^{2-}

The isotope shifts of the 806 cm^{-1} absorption feature (Tab. VI) indicate an assignment to a bending mode of a molecule containing at least carbon and oxygen. From the possible candidates $HCOO^-$ is excluded since the isotope shifts are not in agreement. It appears, however, that the observed shifts are characteristic of the carbonate ion. Sterzel and Chorinsky (1968 [SC68]) reported a ^{13}C isotope shift of 27 cm^{-1} for CO_3^{2-} in calcite, and Ogden and Williams (1981 [OW81]) reported a shift of 10 cm^{-1} for ^{18}O substitution in alkali-metal carbonates. These two values agree with the isotope shifts observed for the 806 cm^{-1} absorption (Tab. VI), and thus we assign this band to the OCO bending mode of the carbonate ion. As a result of the relative weakness of the 806 cm^{-1} absorption feature, we expect that the contribution of the stronger C=O stretching mode of CO_3^{2-} (which can be anywhere between 1400 and 1500 cm^{-1} : SC68 ; OW81), to our IR spectra is little, although we are not able to quantify this amount.

3.3.2 *Temperature induced changes.* — As discussed before, heating generally resulted in the appearance and disappearance of absorption bands (Tab. VI). Once H_2O had sublimated most ot the remaining bands could clearly

be distinguished. It is remarkable to see how well the absorption bands are resolved when compared with the IR spectra reported by dH86 and S88. In their residue spectra severe blending of IR absorption bands occured which is the result of the much longer irradiation times (> 24 hr) and different sample compositions.

To study the effect of sublimation in some detail, we have recorded IR spectra after discrete time intervals at sample temperatures of 176, 216, 228 and 242 K. Figure 13 shows the IR spectra recorded at 176 K. Rapid H_2O sublimation occurred at this temperature. Vapor pressure equilibrium calculations give an H_2O evaporation rate of 2×10^{-3} μm s^{-1} at 173 K (Grim and Greenberg, 1987a) so that three hours of annealing was sufficient to sublimate all H_2O. It is interesting to note that at 176 K the peak positions were not affected by H_2O sublimation. For example, the NH_4^+ position remained at 1454 cm^{-1} which is important for the understanding of the interstellar 6.86 μm (1458 cm^{-1}) absorption feature (Grim *et al.*, 1989b).

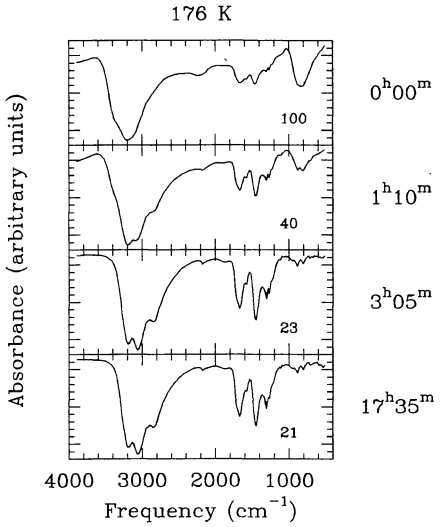

FIGURE 13. — The effect of annealing at 176 K : H_2O sublimation from the irradiated $H_2O/NH_3/CO/O_2 = 10/1/1/1$ mixture. Note that no frequency shifts are observed. The intensity scaling factor 100 in the top figure corresponds to the factor 26 in figure 9.

The effects of further heating are illustrated in figure 14. At 196 K the NH_4^+ absorption band shifted to a lower frequency (1447 cm^{-1}) where it remained even after a further temperature rise. At 196 K, however, on a time scale of one day, a significant fraction of the $NH_4^+X^-$ had sublimated as HX and NH_3. The evaporation on longer time scales was not investigated, but it merits a further study in relation to the survival of these salt-like residues in the interstellar medium.

3.4 UV IRRADIATION OF $AR/NH_3/O_2$ MIXTURES. — The previous sections presented the results of UV irradiation of

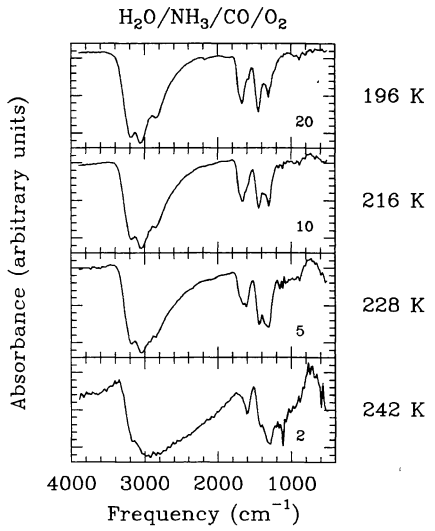

FIGURE 14. — Temperature induced spectral effects after irradiation of the $H_2O/NH_3/CO/O_2 = 10/1/1/1$ mixture. The intensity scaling factors are given with respect to the spectrum taken at 176 K at 0h00m (Fig. 13).

simple binary, and more complex, molecular ices. The products seen in these ices were the *ultimate* result of numerous reactions induced by the ultraviolet photons. Because in ices the reactants were *direct* neighbors, intermediate species were not stored and hence not observed. In an attempt to investigate the *intermediate* reactions we have performed additional irradiation experiments with NH_3/O_2 and NH_3/CO mixtures diluted in argon. In the argon matrix at 12 K, the initially formed photoproducts would be stabilized and by slow evaporation of the argon matrix, we should be able to monitor, step by step, the formation of the intermediate and final species. After sublimation of the argon a comparison could be made with the results from the irradiated binary ices in order to check if the end products in the argon matrices were similar to the end products in the binary ices. If so, the extrapolation from the observed reaction scheme in argon matrices to the dirty ices is justified.

We have photolyzed an $Ar/NH_3/O_2$ mixture with a 300/1/1 composition. After each irradiation interval (total UV times 10m, 30m, 1h, 2h, 4h and 19h) IR spectra were recorded. Subsequently, the sample was annealed to 20, 24, 30 (1h), 33 (2h), 36 (1h) and 40 K (30m), respectively. Annealing times are noted in parenthesis. At each temperature, diffusion and reactions were monitored by taking IR spectra at various times. The results are displayed in figure 15 where the IR spectra taken after deposition, UV irradiation (19h), and warm up to 36 and 40 K are shown. The assignments of the absorptions are given in table VII. The temperature/time range in this table indicates the appearance and disappearance of the absorption in the IR spectra.

3.4.1 *Initial photoproducts.* — With the initiation of the UV irradiation, the NH_3 bands decreased in strength. Four

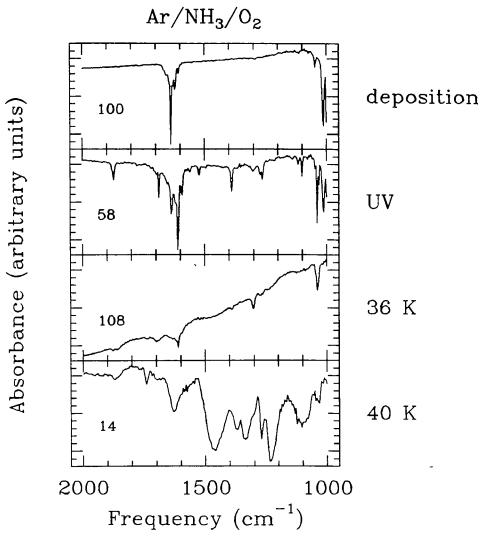

FIGURE 15. — The 2000 – 1000 cm^{-1} IR spectra of an $Ar/NH_3/O_2 = 300/1/1$ mixture after deposition, UV irradiation, and heating to 36 and 40 K. Note that at 36 K the IR spectrum is severely affected by scattering induced by argon sublimation. At 40 K all argon has disappeared.

new absorptions appeared after 30m of UV. The 1040 and 1119 cm^{-1} bands resulted from ozone. The 1389 cm^{-1} band is readily assigned to the HO_2 radical, whereas the assignment of the 1522 cm^{-1} band is not straightforward. Its position points to an OH_x or NH_x bending vibration, but to our knowledge no simple radical shows an absorption at this place in argon matrices. The following two assignments for the 1522 cm^{-1} feature were considered :

(i) *Hydroxylamine* – NH_2OH

If O_3 and HO_2 were immediately produced by the reaction of an oxygen and a hydrogen atom with O_2 in an argon cage, a similar scheme could account for the 1522 cm^{-1} absorption. In this case, a photochemically produced oxygen atom is required to migrate to a cage containing an NH_3 molecule. The kinetic energy of the oxygen atom after dissociation breaks an N–H bond in NH_3 and the oxygen atom then reacts with the hydrogen atom. Due to the cage effect the OH radical cannot escape and it will recombine with NH_2 to form hydroxylamine, NH_2OH. Unfortunately, no spectra of NH_2OH isolated in argon are available in the literature to test this supposition. It should be noted that NH_2OH vapor shows prominent absorption bands at 1115, 1125, 1357 and 1605 cm^{-1}, which do not agree in position and strength with the absorptions seen in the irradiated $Ar/NH_3/O_2$ matrix.

(ii) *The* $(Ar_nH)^+NH_2^-$ *complex*

The formation of this complex is indirectly indicated by the appearance of several absorptions which can be assigned to charged complexes with argon. After 19h UV we observed a very weak band at 906 cm^{-1}.This band was also observed after discharge depositions (Bondybey and Pimentel, 1972) and Lyman α irradiation of argon matrices containing sources for hydrogen atoms (MJ73; van IJzendoorn *et al.*, 1983 ; van der Zwet, 1986). It was assigned to the $(Ar_nH)^+$ complex (MJ73). In the $Ar/NH_3/O_2$ experiment, the $(Ar_nH)^+$ feature disappeared after warming to 20 K, but subsequently new features at 1350 and 1368 cm^{-1} appeared. In a matrix isolation study of alkali metals interacting with NO, absorptions at 1350 and 1375 cm^{-1} were assigned to an NO^- ion in a complex with the alkali metal (MJ71). It is templing to assign the 1350 and 1368 cm^{-1} absorptions to an $(Ar_nH)^+NO^-$ complex, especially since these absorptions vanished with the evaporation of argon (Tab.VII). In addition to this indirect reasoning, we know from the literature that the NH_2 bending mode of the NH_2^- ion in alkali amides is between 1505 and 1556 cm^{-1} (von Müller *et al.*, 1969). Taken together, the assignment of the 1522 cm^{-1} absorption to the $(Ar_nH)^+NH_2^-$ complex is the best of the two alternatives. The charge of the NH_2^- ion accounts for the frequency shift observed with respect to the absorption frequency of NH_2 (1500 cm^{-1} : MJ65).

Other photoproducts that are observed after UV irradiation include O_3, H_2O, H_2O_2, NH_2, NO, NO_2, NO_3, HNO, HNO_2 and HNO_3. We have not observed OH (Acquista *et al.*, 1968), whereas absorptions from matrix isolated H_2O (1599 and 3720 cm^{-1}) and H_2O_2 (1276 and, possibly, 3412 and 3568 cm^{-1}) have been detected.

3.4.2 *Warm up products.* — Mild heating of the argon matrix permitted slow diffusion of the trapped species. Compounds formed during the first heating step to 20 K included the $(Ar_nH)^+NO^-$ complex. After heating to 33 and 36 K a few interesting changes occured (Fig. 15). First, the absorption bands due to HNO and HNO_2 decreased in strength, while a band at 1244 cm^{-1}, assigned to NO_2^-, appeared. By far the most interesting spectral changes were observed after heating to 40 K, the tempereature where argon sublimation was rapid. The HNO, HNO_2 and HNO_3 absorption bands had completely disappeared and were replaced by new bands. The NO_2^- and H_2O_2 bands shifted to lower frequency (Fig.15). The new bands are assigned to NO_3^- (2x), NH_4^+ and N_xO_y on the basis of the results presented in section 3.1. That irradiation and heating of the $Ar/NH_3/O_2 = 300/1/1$ mixture ultimately led to the same species as the observed in the $NH_3/O_2 = 1/1$ ice mixture (Sect. 3.1) is shown by the comparison in figure 16.

3.5 UV IRRADIATION OF $Ar/NH_3/CO$ MIXTURES. — A similar experiment has been performed with an $Ar/NH_3/CO$ mixture. We limit our discussion of the $Ar/NH_3/CO = 300/1/1$ mixture to its most salient aspects. The results of photolysis and heating of the mixture are shown in figure 17. During UV irradiation new bands grew in that are assigned to HCO (1861 cm^{-1}), NH_2CO (1839 cm^{-1}), NCO (1960 cm^{-1}), $HCONH_2$ (1720 cm^{-1}), HNCO (2260 and 2265 cm^{-1}) and CO_2 (2346 cm^{-1}).

Upon slow warm up the radical bands disappeared and

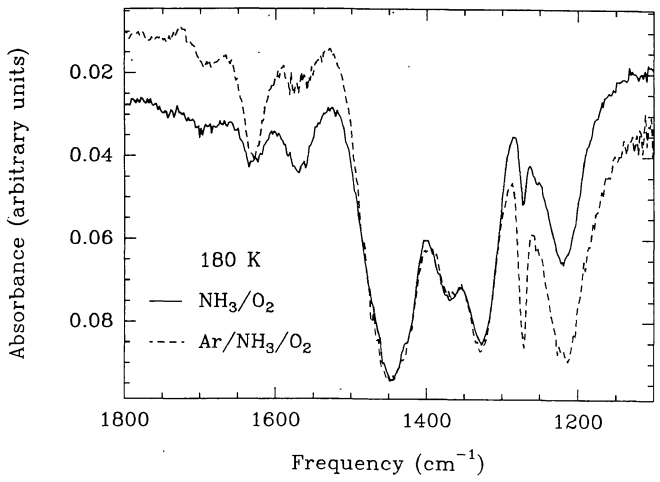

FIGURE 16. — A comparison at 180 K between the 1800 − 1100 cm^{-1} IR spectra of irradiated NH_3/O_2 and $Ar/NH_3/O_2$ = 300/1/1 demonstrating that the end products in both samples are the same.

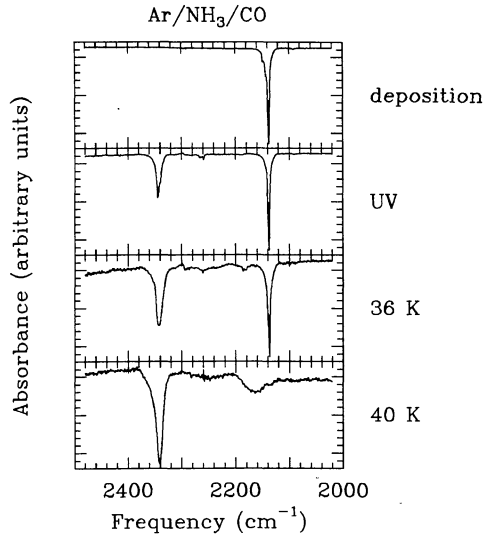

FIGURE 17. — The 2500 − 2000 cm^{-1} IR spectra of an $Ar/NH_3/CO$ = 300/1/1 mixture after deposition, UV irradiation, and heating to 36 and 40 K.

new bands appeared. Furthermore, when argon evaporated the concentration of other species increased as indicated by the dramatic change in shape and position of the NH_3 absorption. But, more interestingly, the HNCO line diminishe and bands at ~ 2185 and ~ 1470 cm^{-1} grew in. After the argon had totally evaporated the 2185 cm^{-1} band had shifte to 2165 cm^{-1} with a FWHM of ~ 40 cm^{-1}. Using the results from section 3.2 we assign the 2165 and 1470 cm^{-1} absorption bands to OCN^- and NH_4^+, respectively. The band positions and widths of the OCN^- and NH_4^+ absorption bands in the annealed argon matrices agree with those in the irradiated NH_3/CO ices.

The conclusion of the last two sections is clear: the argon experiments provide an excellent opportunity to investigate the initial steps in the complex reaction schemes that occur in the irradiated molecular ices. This approach is supported by the fact that the end products in the argon mixtures and in the molecular ices are the same (see Fig. 16).

4. Discussion.

One of the new and interesting results from the experiments described in the previous sections is the formation of ions. It must be noted here that Hagen (1982) already speculated upon this possibility. We consider the ion formation to be promoted by proton transfer reactions. This discussion is largely based on the theory of *solvation* which is reviewed in section 4.2. In section 4.3 we show how this phenomenon is related to our results. Using integrated band strengths we derive the column densities of the molecules and ions for the NH_3/O_2 experiment in section 4.4. From the experimentally observed strength of the NH_4^+ band, we deduce a minimum value for its integrated band strength.

4.1 NEW ASPECTS IN THE PHOTOCHEMISTRY OF ASTROPHYSICAL ICES. — Using the results presented in section 3, we list in tables VIII and IX the reactions leading to the observed species in the NH_3/O_2 and NH_3/CO photolysis experiments. From both tables it is evident that the reaction pathways lead to a wide variety of photoproducts. Since not all products have a permanent dipole or have high enough integrated IR band strengths, the possibility that we overlooked the formation of some products other than those listed cannot be excluded. Both tables start with the photodissociation reactions for first order products (radicals). For the NH_3/CO experiments, these reactions primarily involve NH_3 since the photodissociation threshold energy of CO (111.8 nm ; Okabe, 1978) exceeds that of Lyman α (121.6 nm) which is the threshold of our UV lamp. In the secondary reaction steps, the next generation of radicals and molecules are created, and so on. New aspects in the photochemistry of molecular ices, the proton transfer reactions that lead to ion formation, are given in the bottom lines.

4.2 SOLVATION. — The entire concept of solvation (Dogonadze *et al.*, 1986a,b) is based on the interaction of an *acid* (the proton donor) and a *base* (the proton acceptor) that interact, in a solvent, via a *hydrogen bond*. Hydrogen bonding has been discussed extensively over the last fifty years as one of the most important interactions between molecules, and is still subject to continuing studies. The importance of hydrogen bonding between water ice and bases in the interpretation of the low frequency wing of the OH stretch fundamental of H_2O has been discussed by Hagen *et al.* (1983a). This interaction can be represented by HOH...B, where B stands for the base. Or more generally by AH...B with AH being an acid. Appropriate references to the theory of hydrogen bonding can be found in Hagen *et al.* (1983a).

So far it has been assumed that the hydrogen atom that participates in the bond is localized *on* the acid side.

However, the interaction between an acid and a base is, in fact, an *equilibrium reaction* described as follows :

$$\underset{\text{(I)}}{AH...B} \leftrightarrow \underset{\text{(II)}}{A^{\delta-}...H...B^{\delta+}} \leftrightarrow \underset{\text{(III)}}{A^- ...H^+B} \qquad (A)$$

The classification I, II, and III is taken from Ault *et al.* (1975). In the *gas* phase, the equilibrium can only shift to the right when a *very strong* acid and base are involved. In the *condensed* phase, however, the polar environment can induce a proton transfer from the acid to the base, even for complexes involving *weak* acids and bases (Zundel and Fritsch, 1984, 1986). The dissociation of the base and acid into a positively and negatively charged species involves two steps : first, the formation of the hydrogen bond (I) and, subsequently, the transfer of the hydrogen atom from the acid to the base (III). When B is a molecule containing several hydrogen atoms (e.g., NH_3), more than one hydrogen bond can be formed. In that case it can interact via any one its other hydrogen atoms with another B molecule :

$$B^+H...B \leftrightarrow B^{(1-\delta)+}...H...B^{\delta+} \leftrightarrow B...H^+B \qquad (B)$$

The net result of (A) and (B) is that the acid is dissociated into A^- and a proton which has *"migrated"*. It thus is possible that the HB^+ so produced is effectively at a *non-neighbouring* location with respect to the negative ion. Remember that in principle all reactions are still in equilibrium. For a discussion of such collective proton motion the reader is referred to Zundel and Fritsch (1986).

In the condensed phase, equilibrium (A) shifts to the right with an increasing polarity of the solvent or with a decreasing temperature (Zundel and Fritsch, 1986). Such equilibria have also been spectroscopically investigated using matrix isolation techniques. Ault *et al.* (1975) have studied various interacting molecular complexes in argon. In their classification, the interaction in the $H_2O.HCl$ complex is considered to be a standard hydrogen bond (type I), i.e., the hydrogen atoms is attached to the chlorine atom. In $NH_3.HCl$, the proton is equally shared by ammonia and the chlorine atom (type II). In the case of $(CH_3)_3N.HBr$ and $(CH)_3N.HCl$ complexes, ion pairs are formed (type III). Ault *et al.* also demonstrated clearly how the IR fundamentals of the involved species are affected by these interactions. Finally, we note that the degree of hydrogen bonding can severely affect the IR band strengths (Kurnig *et al.* 1987.; Süzer and Andrews 1987).

For the interpretation of our experimental results the solvation of HNO_3 in H_2O/Ar or NH_3/Ar matrices (RD77b) are the most relevant. In these studies, the HNO_3-to-matrix ratio was kept constant (0.1%), but the $[H_2O]/[Ar]$ and $[NH_3]/[Ar]$ compositions were varied between 0 and 100%. For concentrations $[H_2O]/[Ar] < 6\%$ and $[NH_3]/[Ar] < 3\%$, absorption bands from the $H_2O2.NHO_3$ and $NH_3.NO_3$ complexes were observed. When the concentrations exceeded these two limiting values, the HNO_3 complex bands were replaced by broad, shifted bands resulting from $H_3O^+NO_3^-$ and $NH_4^+NO_3^-$. For the latter, the bands resulted from a split NO_3^- fundamental and a band at 1495 cm^{-1} assigned to the NH_4^+ bending fundamental.

4.3 SOLVATION IN ASTROPHYSICAL ICES. — How does the solvation theory apply to irradiated astrophysical ices? First of all, the presence of NH_3 in the samples is *essential* for the appearance of the ionic absorption features. It is clear that in the irradiated inert matrices and reactive ices NH_3 acts as the base B. The next question is what acids AH are involved? From the solvation theory and the identification of NO_2^-, NO_3^-, OCN^- and NH_4^+ ions, we deduce that they are formed by the interaction of HNO_2, HNO_3 and HNCO with NH_3 (Tabs. VIII and IX). Similarly, interaction of HCN and HCOOH with NH_3 will lead to CN^- and $HCOO^-$ formation. That these acids are indeed the intermediates in the ion formation scheme has been clearly demonstrated by the argon experiments (Sects. 3.4 and 3.5).

In the astrophysically relevant ices, ion formation is observed for NH_3 concentrations as low as 5% (Sect. 3.3). This value is lower than for the binary mixtures (10 – 50% ; Sect. 3.1 and 3.2), but since water molecules are extremely efficient in forming hydrogen bonds, we expect that a very extended network of hydrogen bonds exists in the sample which promotes the proton transfer according to equilibrium (B). To be more specific we give one example with AH=HNCO, B= NH_3 diluted in H_2O :

$$...NH_3...HOH...HOH...HOCN \leftrightarrow$$
$$...NH_3...H...OH...H...OH...H...OCN \leftrightarrow$$
$$...NH_4^+...HOH...HOH...OCN^- \qquad (C)$$

At low temperature ($T < 100$ K) equilibrium (C) leads to a state in which we consider the ions in our samples to be *isolated*, i.e., the positive and negative ions do not form contact pairs.

The spectral changes observed in the irradiated samples after further warm up are explained as follows : In the NH_3/O_2 samples the NH_4^+ bending mode started to shift above 100 K, roughly the NH_3 sublimation temperature. In the astrophysical mixtures, the NH_4^+ bending mode shifted at the onset of H_2O sublimation (170 – 180 K). This implies that the NH_3 or H_2O molecules, intermediate between the ions, disappeared. *Ion contact pairs* were formed, as suggested by the observation of the spectral features due to NH_4NCO and NH_4NO_3. A new equilibrium replaces equilibrium (C) :

$$NH_3...HNCO \leftrightarrow NH_4^+...OCN^- \qquad (D)$$

This equilibrium tends to shift to the left for two reasons: firstly, because of the increased temperature (Zundel and Fritsch, 1986) and, secondly, because once formed NH_3 and HNCO sublime pulling the equilibrium to the left. Indeed NH_4NCO and NH_4NO_3 sublimated as indicated by the measured IR spectra.

4.4 COLUMN DENSITIES AND THE NH_4^+ INTEGRATED BAND STRENGTH. — Ultimately, one is interested in column densities (n_x), IR cross section (σ_x) or, even better, integrated IR band strengths (A_x) of components (x) in the solid phase. Because of the limited available data the results are not always very precise. Person (1981) summarizes the difficulties that are involved in measuring the optical constants of thin condensates. One of the principal sources of errors is the establishment of accurate baselines, especially when blending of absorption lines occurs. It has been estimated that such error might be as great as 30%. dHA86 have performed IR studies on various astrophysically relevant molecules and mixtures and also reported absolute IR band strengths. Yet, for some molecules the IR band strengths are not measured in the condensed phase and, when necessary, one has to assume gas phase values as an approximation (see below). In this section we calculate first column densities by averaging four NH_3/O_2 irradiation experiments and from this we can derive, using the principle of nitrogen conservation, a *minimum* integrated band strength for the NH_4^+ bending mode.

In table X we have tabulated the results of our calculations. The following assumptions have been made : (i) Since no solid phase IR band strengths for NO and N_2O were available, we are forced to use their corresponding gas phase values ; (ii) The N_2O_3/N_2O_4 absorption bands near 1300 cm^{-1} are assumed to have IR band strengths that are between the values of N_2O and N_2O_5 (deMore and Davidson, 1959 ; Pugh and Rao, 1976) and for purposes of arguments $A_{N_2O_3} = A_{N_2O_4} = 0.5$ and 1.0×10^{-16} cm molecule^{-1}, respectively, are used (assumptions a and b) ; (iii) Another important IR band strength value is that of the "umbrella" mode of NH_3 (1050 cm^{-1}). dH86 reported a value of 1.7×10^{-16} cm molecule^{-1} (assumption c). In unpublished IR transmission experiments we have measured a value of 2.7×10^{-16} cm molecule^{-1} (assumption d), while Kurnig *et al.* (1987) calculated a theoretical value of 3.7×10^{-16} cm molecule^{-1}, which according to them is in agreement with the experiments reported by Süzer and Andrews (1987). Applying the last value to our results, however, led to a total number of nitrogen locked in new molecules greater than the amount of NH_3 which has disappeared (ΔNH_3). We must, therefore, reject the last value. As can be seen from table X, the calculations lead to an IR band strength for NH_4^+ in the range of 4×10^{-17} to 4×10^{-16} cm molecule^{-1}. If we consider charge balance, i.e., $n(NH_4^+) = n(NO_2^-) + n(NO_3^-)$, a value of 2×10^{-16} cm molecule^{-1} seems to be the most reasonable value. The large uncertanties involved in this calculation lead to an estimated range of error of about a factor 2.

5. Astrophysical implications and conclusions.

The results presented in this paper concerned new aspects in understanding the photochemistry of astrophysically relevant molecular ices. The complex photochemistry of such ices was simplified by first considering simple binary mixtures. Since many molecular components can contribute to a single band in the IR spectrum, we have used isotopic labelling techniques to constrain the number of possible candidates. In the NH_3/O_2 and NH_3/CO experiments many radicals and molecules have been formed by UV irradiations: NO, N_2O, N_2O_3, N_2O_4, N_2O_5, O_3, NH_2, N_2H_2, N_2H_4, HCO, H_2CO, $CONH_2$, $HCONH_2$ and CO_2 . In the these studies, however, some compounds were not observed, e.g., HNO_3, HNCO, HCOOH. Their absence was *"compensated"* by the appearance of new strong absorption bands at 1233, 1337, 1385, 1497, 1609, and 2157 cm^{-1}. Combining consideration of isotopically induced induced frequency shifts and theoretical arguments, these bands were identified as NO_2^-, NO_3^- (2x), NH_4^+, $HCOO^-$ and OCN^-, respectively. The presence of CN^- and $NH_2CO_2^-$ was also suggested.

Photochemically induced ion formation by *non-ionizing* UV radiation was explained using the theory of solvation. The missing components (HNO_3, HNCO and HCOOH) all have an acidic character ; i.e., they are capable of donating a hydrogen atom to a base. Once formed, the acids interact with ammonia through a hydrogen bond. Next, due to the basic character of ammonia, a proton transfer reaction is induced so that NH_4^+ and the negative ions are formed. At low temperature, collective proton transfer reactions occur as a result of the extended hydrogen bonding network. This ultimately results in what one may consider to be isolated ions. Heating eliminates the intermediate NH_3 (and other components) by sublimation leading to ion contact pairs, e.g., NH_4NCO and NH_4NO_3. Their formation is suggested by a reasonable agreement in spectral properties. UV irradiation experiments with NH_3/O_2 and NH_3/CO mixtures in argon support the reaction mechanism described above and provide important information on intermediate stages during the photolysis experiment.

Experiments using $H_2O/NH_3/CO/O_2$ ices in various ratios were performed to test the astrophysical relevance of this study. Methane, CH_4, was omitted after it appeared that the interstellar absorption features were reproduced after irradiation of the above mentioned ices. By no means do we imply with this omission that methane is not an astrophysically important molecule. Furthermore, the H_2O concentration is not a critical parameter for the ion formation since H_2O is a powerful source of hydrogen bonding. It fully participates in the overall hydrogen bonding network permitting and stimulating the proton tranfer reactions leading to the ion formation.

The aim of this study was to provide a qualitative as well as a quantitative comparison between the laboratory spectral features and those observed towards interstellar objects. The icy mantles that have accreted on the grains in the protostellar cloud show features that cannot be assigned to simple compounds and that are likely to result from energetic photoprocesses. Such comparisons are shown in Grim and Greenberg (1987b) and Grim *et al.* (1989b) for the 4.62 and 6.86 μm absorption features in W33A. We

suggest that these absorptions are likely due to OCN^- and NH_4^+, respectively, in the photoprocessed grain mantles. In table XI, finally, we summarize the spectral features of ions which are astrophysical interest, together with their respective integrated band strengths.

In addition to the OCN^- and NH_4^+ identifications, this study provides an extensive data base for future interpretations of new observations, especially those from spectral intervals that will be accessible with the *Infrared Space Observatory (ISO)*. In particular, a search for CO_2 should yield information on the photoprocessing of interstellar grains since this species cannot be produced by grain surface reactions, but is readily produced by photoprocessing (Grim and d'Hendecourt, 1986). Similarly, CO_2 will also be an indirect tracer for the presence of molecular oxygen in grain mantles, as does NO_2^-. Detection of CH_4 could be important in relation to grain surface recombination processes and the formation of the organic residue mantles (S88). And ultimately, detection of such molecules as NH_4NCO or NH_2CONH_2 (urea) could provide further information about the thermal histories of interstellar grains. Specific details relating our results to *ISO* will be given in a forthcoming paper (Grim and d'Hendecourt, 1989).

References

ACQUISTA N., SCHOEN L.J., and LIDE Jr., D.R. : 1968, *J. Chem. Phys.* **48**, 1534.
AGARWAL V.K., SCHUTTE W., GREENBERG J.M., FERRIS J.P., BRIGGS R., CONNOR S., VAN DE BULT, C.E.P.M., and BAAS F. : 1985, *Origins of Life* **16**, 21.
ALLAMANDOLA L.J. : 1984, *Galactic and Extragalactic Infrared Spectroscopy,* Eds. M.F. Kessler and P.J. Phillips (Dordrecht : Reidel) 5.
AULT B.S., STEINBACK E., and PIMENTEL G.C. : 1975, *J. Phys. Chem.* **79**, 615.
BAAS F., GRIM R.J.A., GEBALLE T.R., SCHUTTE W.A., and GREENBERG J.M. : 1988, *Dust in the Universe,* Eds. M.E. Bailey and D.A. Williams (Cambridge : University Press) 55.
BAR-NUN A., HERMAN G., LAUFER D., and RAPPAPORT M.L. : 1985, *Icarus* **63**, 317.
BAR-NUN A., DROR J., KOCHAVI E., and LAUFER D. : 1987, *Phys. Rev. B* **35**, 2427.
BECKER E.D., and PIMENTEL G.C. : 1956, *J. Chem. Phys.* **25**, 224.
BERCKMANS D., FIGEYS H.P., MARÉCHAL Y., and GEERLINGS P. : 1988, *J. Phys. Chem.* **92**, 66.
BERNITT D.L., HARTMAN K.O., and HISATSUNE I.C. : 1965, *J. Chem. Phys.* **42**, 3553.
BERTIE J.E., and MORRISON M.M. : 1980, *J. Chem. Phys.* **73**, 4832.
BHATIA S.C., and HALL Jr., J.H. : 1980, *J. Phys. Chem.* **84**, 3255.
BONDYBEY V.E., and PIMENTEL G.C. : 1972, *J. Chem. Phys.* **56**, 3832.
BREWER L., and LING-FAI WANG J. : 1972, *J. Chem. Phys.* **56**, 759.
BROOKER M.H., and IRISH D.E. : 1971, *Can. J. Chem.* **49**, 1289.
BUTCHART I., MCFADZEAN A.D., WHITTET D.C.B., GEBALLE T.R., and GREENBERG J.M. : 1986, *Astron. Astrophys.* **154**, L5.
CANTRELL C.A., DAVIDSON J.A., SHETTER R.E., ANDERSON B.A., and CALVERT J.G. : 1987, *J. Phys. Chem.* **91**, 6017.
CATALANO E., SANBORN R.H., and FRAZER J.W. : 1963, *J. Chem. Phys.* **38**, 2265.
CATALANO E., and SANBORN R.H. : 1963, *J. Chem. Phys.* **38**, 2273.
CHADWICK B.M., and EDWARDS H.G.M. : 1973, *A Specialist Periodical Report - Molecular Spectroscopy* - Vol. 1 (London : The Chemical Society) 446.
CHAIKEN R.F., SIBBETT D.J., SUTHERLAND J.E., VAN DE MARK D.K., and WHEELER A. : 1962, *J. Chem. Phys.* **37**, 3211.
DEKOCK R.L., and WELTNER Jr., W. : 1971, *J. Chem. Am. Soc.* **93**, 7106.
DEMORE W.B., and DAVIDSON N. : 1959, *J. Chem. Am. Soc.* **20**, 5869.
D'HENDECOURT L.B., ALLAMANDOLA L.J., and GREENBERG J.M. : 1985, *Astron. Astrophys.* **152**, 130.
D'HENDECOURT L.B., and ALLAMANDOLA L.J. : 1986, *Astron. Astrophys. Suppl. Ser.* **64**, 453.
D'HENDECOURT L.B., ALLAMANDOLA L.J., GRIM R.J.A., and GREENBERG J.M. : 1986, *Astron. Astrophys.* **158**, 119.
DOGONADZE R.R., KÁLMÁN E., KORNYSHEV A.A., and ULSTRUP J. : 1986a, *The Chemical Physics of Solvation : Part A. Theory of Solvation* (Amsterdam : Elsevier).
DOGONADZE R.R., KÁLMÁN E., KORNYSHEV A.A., and ULSTRUP J. : 1986b, *The Chemical Physics of Solvation : Part B. The Chemical Physics of Solvation* (Amsterdam : Elsevier).
DUBOST H. : 1976, *Chem. Phys.* **12**, 139.
DUBOST H., CHARNEAU R., and HARIG M. : 1982, *Chem. Phys.* **69**, 389.
FALK M. : 1987, *J. Chem. Phys.* **86**, 560.
FATELEY W.G., BENT H.A., and CRAWFORD Jr., B. : 1959, *J. Chem. Phys.* **31**, 204.
FERRARO J.R., SILL G., and FINK U. : 1980, *Applied Spectr.* **34**, 525.
FRASCO D.L. : 1964, *J. Chem. Phys.* **44**, 2134.
GEBALLE T.R., BAAS F., GREENBERG J.M., SCHUTTE W. : 1985, *Astron. Astrophys.* **146**, L6.
GEBALLE T.R. : 1986, *Astron. Astrophys.* **162**, 248.
GEBALLE T.R., KIM Y.H., KNACKE R.F., NOLL K.S. : 1988, *Astrophys. J. Lett.* **326**, L65.
GREENBERG J.M. : 1971, *Astron. Astrophys.* **12**, 240.
GREENBERG J.M. : 1982a, *Comets,* Ed. L.L. Wilkening (Tucson : University of Arizona Press) 131.
GREENBERG J.M. : 1982b, *Submillimetre Wave Astronomy,* Eds. J.E. Beckman and J.P. Phillips, (Cambridge : University Press) 261.

GREENBERG J.M., VAN DE BULT, C.E.P.M., and ALLAMANDOLA L.J. : 1983, *J. Phys. Chem.* **87**, 4243.
GREENBERG J.M., GEBALLE T.R., BAAS F., HAGE J. : 1988, in preparation.
GRIM R.J.A., and D'HENDECOURT L.B. : 1986, *Astron. Astrophys.* **167**, 161.
GRIM R.J.A., and GREENBERG J.M. : 1987a, *Astron. Astrophys.* **81**,155.
GRIM R.J.A., and GREENBERG J.M. : 1987b, *Astrophys. J. Lett.* **321**, L91.
GRIM R.J.A. : 1988, *The Photochemical and Thermal Evolution of Interstellar and Cometary Ices* (University of Leiden) Ph. D. Thesis.
GRIM R.J.A., GEBALLE T.R., BAAS F., and GREENBERG J.M. : 1989a, submitted to *Astron. Astrophys.*
GRIM R.J.A., GREENBERG J.M., SCHUTTE W.A., and SCHMITT B. : 1989b, submitted to *Astrophys. J. Lett.*
GRIM R.J.A., and D'HENDECOURT L.B. : 1989, in preparation for *Astron. Astrophys.*
GUILLORY W.A., and HUNTER C.E. : 1969, *J. Chem. Phys.* **50**, 3516.
GUILLORY W.A., and HUNTER C.E. : 1971, *J. Chem. Phys.* **54**, 598.
GUILLORY W.A., and BERNSTEIN M.L. : 1975, *J. Chem. Phys.* **62**, 1058.
HAGEN W., ALLAMANDOLA L.J., and GREENBERG J.M. : 1979, *Astrophys. Space Sci.* **65**, 215.
HAGEN W., TIELENS A.G.G.M., and GREENBERG J.M. : 1981, *Chem. Phys.* **56**, 367.
HAGEN W. : 1982, *Chemistry and Infrared Spectroscopy of Interstellar Grains* (Univeristy of Leiden) Ph. D. Thesis.
HAGEN W., TIELENS A.G.G.M., and GREENBERG J.M. : 1983a, *Astron. Astrophys. Suppl. Ser.* **51**, 389.
HAGEN W., TIELENS A.G.G.M., and GREENBERG J.M. : 1983b, *Astron. Astrophys.* **117**, 132.
HALL R.T., and PIMENTEL G.C. : 1963, *J. Chem. Phys.* **38**, 1889.
HAMMAKER R.M., and WALTERS J.P. : 1964, *Spectrochim. Acta* **20**, 1311.
HARTMAN K.O., and HISATSUNE I.C. : 1966, *J. Chem. Phys.* **44**, 1913.
HODAPP K.-W., SELLGREN K., and NAGATA T. : 1988, *Astrophys. J. Lett.* **326**, L61.
HUBBARD J.S., VOECKS G.E., HOBBY G.L., FERRIS J.P., WILLIAMS E.A., and NICODEM D.E. : 1975, *J. Mol. Evol.* **5**, 223.
ITO K., and BERNSTEIN H.J. : 1956, *Can. J. Chem.* **34**, 170.
IRISH D.E., and DAVIS A.R. : 1968, *Can. J. Chem.* **46**, 943.
IRVINE M.J., MATHIESON J.G., and PULLIN A.D.E. : 1982, *Aust. J. Chem.* **35**, 1971.
ISMAIL Z.K., HAUGE R.H., and MARGRAVE J.L. : 1973, *J. Mol. Spectr.* **45**, 304.
JACOX M.E., and MILLIGAN D.E. : 1964, *J. Chem. Phys.* **40**, 2457.
JACOX M.E., MILLIGAN D.E., MOLL N.G., and THOMPSON W.E. : 1965, *J. Chem. Phys.* **43**, 3734.
JACOX M.E., and MILLIGAN D.E. : 1972, *J. Mol. Spectr.* **42**, 495.
JACOX M.E., and MILLIGAN D.E. : 1973, *J. Mol. Spectr.* **48**, 536.
JACOX M.E., and MILLIGAN D.E. : 1974, *Chem. Phys. Lett.* **28**, 163.
KAFAFI Z.H., HAUGE R.H., BILLUPS W.E., and MARGRAVE J.L. : 1984, *Inorganic Chem.* **23**, 177.
KATO R., and ROLFE J. : 1967, *J. Chem. Phys.* **47**, 1901.
KELLER W.E., and HALFORD R.S. : 1949, *J. Chem. Phys.* **17**, 26.
KING C.M., and NIXON E.R. : 1968, *J. Chem. Phys.* **48**, 1685.
KING S.T. : 1971, *J. Phys. Chem.* **75**, 405.
KITTA K., and KRÄTSCHMER W. : 1983, *Astron. Astr.* **122**, 105.
KNACKE R.F., MCCORKLE S., PUETTER R.C., ERICKSON E.F., and KRÄTSCHMER W. : 1982, *Astrophys. J.* **260**, 141.
KNACKE R.F., and MCCORKLE S. : 1987, *Astron. J.* **94**, 972.
KURNIG I.J., SZCZĘŚNIAK M.M., and SCHNEIDER S. : 1987, *J. Chem. Phys.* **87**, 2214.
LACY J.H., BAAS F., ALLAMANDOLA L.J., PERSSON S.E., MCGREGOR P.J., LONSDALE C.J., GEBALLE T.R., and VAN DE BULT C.E.P.M. : 1984, *Astrophys. J.* **276**, 533.
LARSON H.P., DAVIS D.S., BLACK J.H., and FINK U. : 1985, *Astrophys. J.* **299**, 873.
LÉGER A., KLEIN J., DE CHEVEIGNE S., GUINET C., DEFOURNEAU D., and BELIN M. : 1979, *Astron. Astrophys.* **79**, 256.
LÉGER A., GAUTIER S., DEFOURNEAU D., and ROUAN D. : 1983, *Astron. Astrophys.* **117**, 164.
LEVINE S.Z., and CALVERT J.G. : 1977, *Chem. Phys. Lett.* **46**, 81.
MILLIGAN D.E., and JACOX M.E. : 1963, *J. Chem. Phys.* **38**, 2627.
MILLIGAN D.E., and JACOX M.E. : 1964, *J. Chem. Phys.* **41**, 3032.
MILLIGAN D.E., and JACOX M.E. : 1965, *J. Chem. Phys.* **43**, 4487.
MILLIGAN D.E., and JACOX M.E. : 1967a, *J. Chem. Phys.* **47**, 278.
MILLIGAN D.E., and JACOX M.E. : 1967b, *J. Chem. Phys.* **47**, 5157.
MILLIGAN D.E., and JACOX M.E. : 1969, *J. Chem. Phys.* **51**, 1952.
MILLIGAN D.E., JACOX M.E., and GUILLORY W.A. : 1970, *J. Chem. Phys.* **52**, 3864.
MILLIGAN D.E., and JACOX M.E. : 1971, *J. Chem. Phys.* **55**, 3404.
MILLIGAN D.E., and JACOX M.E. : 1973, *J. Mol. Spect.* **46**, 460.
MOLL N.G., CLUTTER D.R., and THOMPSON W.E. : 1966, *J. Chem. Phys.* **45**, 4469.
MORRIS V.R., BHATIA S.C., and HALL Jr., J.H. : 1987, *J. Phys. Chem.* **91**, 3359.
MUKAI T., and KRÄTSCHMER W. : 1986, *Earth, Moon and Planets* **36**, 145.
NAKAMOTO K. : 1986, *Infrared and Raman Spectra of Inorganic and Coordination Compounds,* 4thEd. (New York : Wiley and Sons).
NARAYANAMURTI V., SEWARD W.D., and POHL R.O. : 1966, *Phys. Rev.* **148**, 481.
NORMAN C., and SILK J. : 1980, *Astrophys. J.* **238**, 158.
OGDEN J.S., and WILLIAMS S.J. : 1981, *J. Chem. Soc. Dalton* 456.
OGILVIE J.F. : 1967, *Spectrochim. Acta* **23A**, 737.
OKABE H. : 1978, *Photochemistry of Small Molecules* (New York : Wiley and Sons).
PERSON W.B. : 1981, *Matrix Isolation Spectroscopy,* Eds. A.J. Barnes *et al.* (Dordrecht : Reidel) 415.

PINCHAS S., and LAULICHT I. : 1971, *Infrared Spectra of Labelled Compounds (London : Academic Press).*
PRASAD S.S., and TARAFDAR S.P. : 1983, *Astrophys. J.* **267**, 603.
PUGH L.A., and RAO K.N. : 1976, *Molecular Spectroscopy : Modern Research, Vol. II,* Ed. K.N. Rao (New York : Academic Press) 165.
REDING F. and HORNIG D.F. : 1951, *J. Chem. Phys.* **19**, 594.
REDING F. and HORNIG D.F. : 1955, *J. Chem. Phys.* **23**, 1053.
RITZHAUPT G., and DEVLIN J.P. : 1975, *J. Phys. Chem.* **79**, 2265.
RITZHAUPT G., and DEVLIN J.P. : 1977a, *J. Phys. Chem.* **81**, 67.
RITZHAUPT G., and DEVLIN J.P. : 1977b, *J. Phys. Chem.* **81**, 521.
ROSENGREN K., and PIMENTEL G.C. : 1965, *J. Chem. Phys.* **43**, 507.
ROUAN D., OMONT A., LACOMBE F., and FORVEILLE T. : 1988, *Astron. Astrophys.* **189**, L3.
ROUX J.A., and WOOD B.E. : 1983, *J. Opt. Soc. Am.* **73**, 1181.
RUBIN M.B., NOYES R.M., and SMITH K.W. : 1987, *J. Phys. Chem.* **91**, 1618.
SANDFORD S.C., ALLAMANDOLA L.J., TIELENS A.G.G.M., and VALERO G.J. : 1988, *Astrophys. J.* **329**, 498.
SCHETTINO V., and HISATSUNE I.C. : 1970, *J. Chem. Phys.* **52**, 9.
SCHMITT B., GRIM R.J.A., and GREENBERG J.M. : 1988a, *Experiments on Cosmic Dust Analogues - Space Sci. Lib.,* Eds. Bussoletti *et al.* (Dordrecht : Reidel) 259.
SCHMITT B., GRIM R.J.A., and GREENBERG J.M. : 1988b, *Dust in the Universe,* Eds. Bailey M.E. and Williams D.A. (Cambridge : University Press) in press.
SCHMITT B., GREENBERG J.M., and GRIM R.J.A. : 1988c, accepted for publication in *Astrophys. J. Lett.*
SCHUTTE W.A. : 1988, *The Evolution of Interstellar Organic Grain Mantles* (University of Leiden) Ph. D. Thesis.
SEWARD W.D., and NARAYANAMURTI V. : 1966, *Phys. Rev.* **148**, 463.
SILL G., FINK U., and FERRARO J.R. : 1980, *J. Opt. Soc. Am.* **70**, 724.
SMITH Jr. D.F., OVEREND J., SPIKER R.C., and ANDREWS L. 1972, *Spectrochim. Acta* **28A**, 87.
SMITH G.R., and GUILLORY W.A. : 1977, *J. Mol. Spectr.* **68**, 223.
SMITH R.G., SELLGREN K., and TOKUNAGA A.T. : 1988, *Astrophys. J.* preprint.
SPINNER E., and ROWE J.E. : 1979, *Aust. J. Chem.* **32**, 481.
SPOLITI M., CESARO S.N., and MARITI B. : 1973, *J. Chem. Phys.* **59**, 985.
STERZEL W., and CHORINSKY E. : 1968, *Spectrochim. Acta* **24A**, 353.
STEWART J.E. : 1957, *J. Chem. Phys.* **26**, 248.
ST. LOUIS R.V., and CRAWFORD Jr., B. : 1965, *J. Chem. Phys.* **42**, 857.
SÜZER S., and ANDREWS L. : 1987, *J. Chem. Phys.* **87**, 5131.
TIELENS A.G.G.M., HAGEN W. and GREENBERG J.M. : 1983, *J. Phys. Chem.* **87**, 4220.
TIELENS A.G.G.M., ALLAMANDOLA L.J., BREGMAN J., GOEBEL J., D'HENDECOURT L.B., and WITTEBORN F.C. : 1984, *Astrophys. J.* **287**, 697.
TIELENS A.G.G.M., and ALLAMANDOLA L.J. : 1987, *Physical Processes in the Interstellar Medium,* Eds. G.E. Morfill and M. Scoler (Dordrecht : Reidel).
VAN DE BULT, C.E.P.M., GREENBERG J.M. and WHITTET D.C.B. : 1985, *Mon. Not. R. Astron. Soc.* **214**, 289.
VAN DER ZWET G.P. : 1986, *A Spectroscopic Study of Absorption and Emission Features of Interstellar Dust Components* (University of Leiden) Ph. D. Thesis.
VAN DER ZWET G.P., ALLAMANDOLA L.J., BAAS F., and GREENBERG J.M. : 1988, accepted for publication in *J. Mol. Struct.*
VAN IJZENDOORN L.J., ALLAMANDOLA L.J., BAAS F., and GREENBERG J.M. : 1983, *J. Chem. Phys.* **78**, 7019.
VAN THIEL M., BECKER E.D., and PIMENTEL G.C. : 1957, *J. Chem. Phys.* **27**, 486.
VARETTI E.L., and PIMENTEL G.C. : 1971, *J. Chem. Phys.* **55**, 3813.
VERDERAME F.D., NEBGEN J.W., and NIXON E.R. : 1963, *J. Chem. Phys.* **39**, 2274.
VERDERAME F.D., and NIXON E.R. : 1966, *J. Chem. Phys.* **44**, 43.
VON MÜLLER A., KEBABCIOGLU R., KREBS B., BOUCLIER P., PORTIER J., and HAGENMULLER P. : 1969, *Z. Anorg. All. Chem.* **368**, 31.
WAGNER E.L., and HORNIG D.F. : 1950a, *J. Chem. Phys.* **18**, 296.
WAGNER E.L., and HORNIG D.F. : 1950b, *J. Chem. Phys.* **18**, 305.
WEAST R.C. : 1983, *CRC Handbook of Chemistry and Physics,* 64th Ed. (Florida : CRC Press).
WEISSBERGER E., BRECKENRIDGE W.H., and TAUBE H. : 1967, *J. Chem. Phys.* **47**, 1764.
WILLNER S.P., GILLETT F.C., HERTER T.L., JONES B., KRASSNER J., MERRILL K.M., PIPHER J.L., PUETTER R.C., RUDY R.J., RUSSELL R.W. SOIFER B.T. : 1982, *Astrophys. J.* **253**, 174.
ZHAO N.S. : 1988, unpublished results.
ZUNDEL G., and FRITSCH J. : 1984, *J. Phys. Chem.* **88**, 6295.
ZUNDEL G., and FRITSCH J. : 1986, *The Chemical Physics of Solvation : Part B. Spectroscopy of Solvation,* Eds. R.R. Dogonadze *et al.* (Amsterdam : Elsevier) 21.

1989A&AS...78..161G

TABLE I. — *Interstellar infrared absorption features.*

λ (μm)	ν(cm^{-1})	Object	Assignment	Reference
2.97	3367	IRAS 09371+1212	H_2O cryst.	9
3.08	3247	protostars (W33A, BN, etc.), obscured field stars, OH/IR stars	H_2O	1
3.38	2959	Galactic Centre, OH 01-477	$-CH_2$	5
3.42	2924	Galactic Centre, OH 01-477	$-CH_3$	5
3.53	2833	W33A	CH_3OH	10
3.95	2532	W33A	H_2S	4
4.617	2166	W33A, NGC 7538/IRS 9	OCN^-	7
4.675	2139	protostars (W33A, etc.), obscured field stars	CO	2 6
4.9	2041	W33A	OCS, XCS	4
5.5	1818	NGC 7538/IRS 9	?	8
6.0	1667	protostars (W33A, etc.)	H_2O	3
6.86	1457	protostars (W33A, etc.)	NH_4^+	11
7.6	1315	NGC 7538/IRS 9	?	8

Note: This table lists an arbitrary selection of interstellar absorption features and objects. The assignments given in column 4 are based on our general work. Other explanations for some of the IR features can be found, e.g., in reference 8.

References.- (1) Léger et al. 1979; (2) Lacy et al. 1984; (3) Tielens et al. 1984; (4) Geballe et al. 1985; (5) Butchart et al. 1985; (6) Geballe 1986; (7) Grim and Greenberg 1987b; (8) Tielens and Allamandola 1987; (9) Geballe et al. 1988; (10) Baas et al. 1988, Grim et al. 1989a; (11) Grim et al. 1989b.

TABLE II. — *Peak frequencies, isotope shifts and assignments of new bands in irradiated $NH_3/O_2 = 1/1$ ices.*

		$NH_3/O_2 = 1/1$[d]			Literature			
Assignment	ν	$\Delta^{15}N$	$\Delta^{18}O$	ΔD	$\Delta^{15}N$	$\Delta^{18}O$	ΔD	Reference
N_2O_4	752[b]	-2	-4	0	6	-3	0	1, 2
NO_2^-	793[a]	0	33		5	38	0	3
	787[b]	12	31	8	5	38	0	3
NO_3^-	820[a]				23	11	0	3
	829[b]	23	11	9	23	11	0	3
N_2O_3	959[a]	8	41		14	24	0	7
	947[b]	13	35	-2	14	24	0	7
O_3	1042[a]		62	6	0	58	0	8, 10
NO_2^-	1233[a]	24	24	2	25	25	0	3, 5
	1219[b]	26	23		26	25	0	3, 5
N_2O_3	1302[a]	14		-5	16	45	0	7
	1273[b]	14	46	-6	16	45	0	7
NO_3^-	1337[a]	31	22	0	31	20	0	3, 11
	1327[b]	35	15		31	20	0	3, 11
NO_3^-	1385[a]	27	17		31	20	0	3, 11
	1370[b]	27	14		31	20	0	3, 11
NH_4^+	1497[a]	18[e]	0		1	0	380[c]	6, 11
	1449[b]	6	-7	377	1	0	380[c]	6, 11
HONO	1599[a]	23	35	-6	29	34		6
	1570[b]	29	35	-6	29	34		6
N_2O_3	1632[b]	37	25	-4	35	31	0	7
N_2O_5	1701[a]			0			0	1
	1703[b]	0	6	-1			0	1
NO	1875[a]	31	46	0	32	47	0	2, 4
N_2O	2236[a]	72	8	0	70	7	0	9

References.- (1) Fateley et al. 1959; (2) Guillory and Hunter 1969; (3) Kato and Rolfe 1967; (4) Milligan and Jacox 1967b; (5) Milligan and Jacox 1971; (6) Pinchas and Laulicht 1971; (7) Varetti and Pimentel 1971; (8) Brewer and Ling-Fai Wang 1972; (9) Smith et al. 1972; (10) Spoliti et al. 1973; (11) Ritzhaupt and Devlin 1977b; (12) Morris et al. 1987.

Notes:

a) Peak frequency and isotope shift measured at 12 K.

b) Peak frequency and isotope shift measured at 180 K.

c) Average value taken from reference 6.

d) The estimated error in the observed frequency shifts is 4 cm^{-1}.

e) This large value is not fully understood, underlying absorption by other nitrogen-oxygen containing photolysis products are a possible reason for this apparent shift, especially since the ^{15}N shifts for this particular band in other experiments was negligible (see Table 3 and 6).

1989A&AS...78..161G

TABLE III. — *Observed peak frequencies of new bands in irradiated and labelled* $NH_3/CO = 1/1$ *ices.*

$\nu(cm^{-1})$		$\nu(cm^{-1})$		$\nu(cm^{-1})$	
$^{14}NH_3/^{12}CO$		$^{14}NH_3/^{13}CO$		$^{15}NH_3/^{12}CO$	
12 K	180 K	12 K	180 K	12 K	180 K
1109[a]	1090				
	1132		1098		1100
1329	1323	1306	1290	1309	1308
1391	1389	1385	1383	1389	1389
1499	1449	1501	1466	1497	1466
1559[a]	1553			1565[a]	
	1609	1574	1597		1607
1697	1684	1676[a]	1657	1692	1676
1840				1844	
1854				1858	
2045					
2076		2031[a]			
	2100[a]			2060	2075
2155	2158	2100[a]	2100	2141[a]	2139
	2214[b]		2160[b]		
2276	2274	2261			
2344		2278		2342	

a) *Value measured from difference spectrum*
b) *Value measured at* $T > 180$ *K (see Figure 11)*

TABLE V. — *Molecules identified in irradiated* NH_3/CO *ices with infrared or mass spectroscopy.*

Species	Formula	IR[a]	GC/MS[b]
	HCO	x	0
	NH_2CO	x	0
Isocyanic acid	HNCO	x	0
Formamide	$HCONH_2$	x	0
Ammonium ion	NH_4^+	x	0
Cyanate ion	OCN^-	x	0
Urea	NH_2CONH_2	x	x
Ammonium cyanate	NH_4NCO	x	0
Oxamide	$NH_2COCONH_2$	0	x
Biuret	$NH_2CONHCONH_2$	0	x

Note: Compounds identified in the GC/MS study that resulted from air contamination have been omitted. Compounds marked with x (0) were (not) observed.

a) *Present work; Schutte 1988*
b) *Agarwal et al. 1985; Schutte 1988*

TABLE IV. — *Observed peak frequencies and assignments of irradiated* NH_3/CO *ices.*

$\nu(cm^{-1})$[a]						
Hagen (1982)		This work			Assignment	
1/3	1/33	10/1	1/1	1/10	Hagen (1982)	This work
	1091		1090[b]		HCO	N_2H_4 (?)
	1134		1132[b]		?	$NH_2CO_2^-$ (?)
1266	1266				$HCONH_2$	
1290	1290			1300	N_2H_2	N_2H_2
1315	1315			1306	N_2H_2	N_2H_2
		1327	1329			$HCONH_2$
1388		1389	1391		NH_4^+	$HCONH_2$
1497	1497	1514	1499		NH_2CONH_2	NH_4^+
	1499			1497	H_2CO	H_2CO, NH_2
		1555[b]	1553[b]			$NH_2CO_2^-$ (?)
		1614[b]	1609[b]			HCO_2^- (?)
1697		1695	1697	1699	NH_2CONH_2	$HCONH_2$
1715	1715				$HCONH_2$	
	1725			1724	$HCONH_2$	$HCONH_2$
	1737			1736	H_2CO	H_2CO
1845	1845		1840		$CONH_2$	$CONH_2$
	1859		1854	1859	HCO	HCO
	1889			1888	NCCO	NCCO
	1937			1937	NCO	NCO
				2028		HNC (?)
			2045			CN (?)
			2076			CN^-, HCN (?)
			2100[b]			CN^-, HCN (?)
2171		2157[b]	2157[b]		?	OCN^-
			2214[c]			NH_4NCO
	2246			2243	HNCO	C_3O_2[d]
2263	2263			2263	HNCO	HNCO
	2281		2276	2278	$^{13}CO_2$	$^{13}CO_2$[d]
2289	2289			2290	HOCN	HOCN
2347	2347	2342	2344	2346	CO_2	CO_2[d]

Notes: a) *Measured at 12 K;* b) *Measured at 180 K;* c) *Measured at 230 K;* d) *Also observed in irradiation of pure CO.*
For comments and references see text.

1989A&AS...78..161G

TABLE VII. — *Observed peak frequencies and assignments of new bands in irradiated* $Ar/NH_3/O_2 = 300/1/1$.

ν (cm^{-1})	first	last	Assignment	Reference
666	12 K (19h)	33 K	CO_2 [b]	24
710	12 K (19h)	36 K (1h)	O_3	14, 17
797	12 K (19h)	33 K (2h)	trans-HNO_2	3, 11
851	12 K (4h)	33 K (2h)	cis-HNO_2	3, 11
905	12 K (19h)	12 K (19h)	$(Ar_nH)^+$	18
1040	12 K (30m)[a]	40 K (30m)	O_3	14, 17
1101	12 K (1h)	33 K (1h)	HO_2, HNO	4, 15
1119	12 K (30m)	33 K (2h)	O_3	14, 17
1242	33 K (20m)	200 K	NO_2^- [c]	10, 12
1265	12 K (2h)	36 K	cis-HNO_2	3, 11
1273	12 K (19h)	200 K	H_2O_2	5, 8
1302	12 K (19h)	36 K (1h)	HNO_3	20
1339	40 K	200 K	NO_3 [c]	22
1350	20 K	36 K (1h)	$(Ar_nH)^+NO^-$	12
1368	30 K	33 K (75m)	$(Ar_nH)^+NO^-$	12
1371	40 K	200 K	NO_3 [c]	22
1389	12 K (30m)	36 K (25m)	HO_2	4, 15
1466	40 K	200 K	NH_4^+	22
1497	12 K (19h)	33 K	NH_2	6
1522	12 K (30m)	24 K	$(Ar_nH)^+NH_2^-$	25
1562	12 K (2h)	33 K (75m)	HNO	19
1593	12 K (2h)	36 K (25m)	H_2O	1
1612	12 K (1h)[a]	?	NO_2	7
1628	40 K	200 K	N_2O_3	13
1634	?	36 K	cis-HNO_2	3, 11
1688	12 K (2h)	36 K	trans-HNO_2, HNO_3	3, 11, 20
1699	33 K (40m)	160 K	N_2O_5 [c]	2
1740	33 K (75m)	120 K	N_2O_4	7
1767	40 K	120 K	N_2O_4	7
1834	30 K	33 K (75m)	$(NO_2)_2$, NO_3, N_2O_3	23, 26
1871	12 K (2h)	120 K	NO, $(NO_2)_2$	2, 9
2108	12 K (19h)	36 K (1h)	O_3	14, 17
2143	12 K (19h)	33 K (1h)	CO [b]	21
2234	24 K	160 K	N_2O	16
2342	12 K (2h)	120 K	CO_2 [b]	24
2717	12 K (19h)	33 K (75m)	HNO	19
3412	12 K (19h)	?	HO_2, H_2O_2	4, 5, 8, 15
3428	12 K (19h)	?	HNO_2 (?)	3, 11
3549	12 K (19h)	?	?	
3568	12 K (19h)	?	H_2O_2	5
3705	12 K (19h)	36 K (45m)	H_2O	1
3727	12 K (19h)	33 K (2h)	H_2O	1

Continued on next page

Notes: The second column indicates the temperature of a first appearance of an absorption line and the third column the last temperature before disappearance. When appropiate, the annealing times are listed in parenthesis, otherwise the spectra are taken immediately after reaching the desired temperature. In the regions 950 – 1100, 1500 – 1600 *and* 3200 – 3500 cm^{-1} *it is particularly difficult to follow the growth and decline of absorption lines because of severe blending with* NH_3 *lines.*

a) Measured from difference spectrum
b) Contaminations from air leak
c) Frequency shifts observed above 40 K are not included (see section 3.1)

References.- (1) van Thiel et al. 1957; (2) Fateley et al. 1959; (3) Hall and Pimentel 1963; (4) Milligan and Jacox 1963; (5) Catalano and Sanborn 1963; (6) Milligan and Jacox 1965; (7) St.Louis and Crawford 1965; (8) Ogilvie 1967; (9) Guillory and Hunter 1969; (10) Milligan et al. 1970; (11) Guillory and Hunter 1971; (12) Milligan and Jacox 1971; (13) Varetti and Pimentel 1971; (14) Brewer and Ling-Fai Wang 1972; (15) Jacox and Milligan 1972; (16) Smith et al. 1972; (17) Spoliti et al. 1973; (18) Milligan and Jacox 1973; (19) Jacox and Milligan 1973; (20) Guillory and Bernstein 1975; (21) Dubost 1976; (22) Ritzhaupt and Devlin 1977b; (23) Bhatia and Hall 1980; (24) Irvine et al. 1982; (25) Nakamoto 1986; (26) Morris et al. 1987.

1989A&AS...78..161G

TABLE VI. — *Observed peak frequencies and assignments of new bands in irradiated and labelled* $H_2O/NH_3/CO/O_2 = 10/1/1/0.25$ *ices.*

$\nu(cm^{-1})$			176 K				
12 K	176 K	196 K	$\Delta(^{13}C)$	$\Delta(^{15}N)$	$\Delta(^{18}O)$	T (K)	Assignment
	806	806	27	0	11	176 – 196	CO_3^{2-}
	887	887	7	0	42	176 – 226	$HCOO^-$
		1231		33	9	118 – 196	NO_2^-
	1263	1273	21	3	38	59 – 216	$HCOO^-$
	1304	1302	25	0	31	98 – 226	$HCOO^-$
	1337		32		64	35 – 216	$HCONH_2$
	1390	1390				35 – 176	$HCONH_2$
1499	1454	1447	0	3	0	12 – 226	NH_4^+
	1580	1584	33	0	14	98 – 226	$HCOO^-$
	1670	1667	32	0	17	12 – 226	$HCONH_2$
1877						12 – 35	NO
	2166	2166	54	12	0	140 – 196	OCN^-
2276						12 – 140	$^{13}CO_2$
2344			66	0	36	12 – 160	$^{12}CO_2$

Note: For comments and references on the assignments see text.

TABLE IX. — *Molecule and ion formation in irradiated* NH_3/CO *ices.*

NH_3	+	$h\nu$	→	$NH_2 + H$	Primary steps
NH_3	+	$h\nu$	→	$NH + H_2$	
CO	+	$h\nu$	→	CO^*	
NH	+	NH_3	→	N_2H_4	Secondary steps
NH	+	NH	→	N_2H_2	
H	+	CO	→	HCO	
NH_2	+	CO	→	$CONH_2$	
NH	+	CO	→	HNCO	
CO	+	CO^*	→	$CO_2 + C$	
$CONH_2$	+	$h\nu$	→	$HNCO + H$	Higher order steps
HCO	+	NH_2	→	$HCONH_2$	
H	+	$CONH_2$	→	$HCONH_2$	
NH_2	+	$CONH_2$	→	NH_2CONH_2	
NH_2	+	$CONH_2$	→	$NH_3 + HNCO$	
$CONH_2$	+	$CONH_2$	→	$NH_2COCONH_2$	
HNCO	+	NH_3	→	$OCN^- \cdots NH_4^+$	Proton transfer reactions
$2NH_3$	+	CO_2	→	$NH_2CO_2^- \cdots NH_4^+$	

For references see Table 8

TABLE VIII. — *Molecule and ion formation in irradiated* NH_3/O_2 *ices.*

NH_3	+	$h\nu$	→	$NH_2 + H$	Primary steps
NH_3	+	$h\nu$	→	$NH + H_2$	
NH_2	+	$h\nu$	→	$NH + H$	
NH	+	$h\nu$	→	$N + H$	
O_2	+	$h\nu$	→	$O + O$	
O	+	H	→	OH	Secondary steps
O	+	NH	→	HNO	
O	+	O_2	→	O_3	
H	+	O_2	→	HO_2	
NH_2	+	O_2	→	$NO + H_2O$	
NH_2	+	OH	→	NH_2OH	Higher order steps
NH_3	+	O	→	NH_2OH	
NH_3	+	OH	→	$NH_2 + H_2O$	
H	+	HO_2	→	H_2O_2	
NO	+	O	→	NO_2	
NO	+	O_2	→	NO_3	
NO_2	+	O	→	NO_3	
NO	+	NO_2	→	N_2O_3	
NO_2	+	NO_2	→	N_2O_4	
NO_2	+	NO_3	→	N_2O_5	
NO	+	N	→	N_2O	
NO	+	NO_2	→	$N_2O + O_2$	
OH	+	NO	→	HNO_2	
OH	+	NO_2	→	HNO_3	
H	+	NO_2	→	HNO_2	
H	+	NO_3	→	HNO_3	
HNO	+	O	→	HNO_2	
HNO	+	O_2	→	HNO_3	
HNO	+	HNO	→	$N_2O + H_2O$	
NH_2	+	NO_2	→	$N_2O + H_2O$	
HNO_2	+	NH_3	→	$NO_2^- \cdots NH_4^+$	Proton transfer reactions
HNO_3	+	NH_3	→	$NO_3^- \cdots NH_4^+$	

References.- de More and Davidson (1959), Hubbard et al. (1975), Levine and Calvert (1977), Hagen (1982), Agarwal et al. (1985), Cantrell et al. (1987), Rubin et al. (1987), Schutte (1988) and results presented in this paper.

1989A&AS...78..161G

TABLE X. — *Column densities in irradiated* $NH_3/O_2 = 1/1$ *ices at 12 K and estimate of the integrated infrared band strength of* NH_4^+

Species x	ν (cm^{-1})	A_x (cm molecule^{-1})	$\int_{\nu_1}^{\nu_2} \tau_\nu \, d\nu$ (cm^{-1})	n_x ($10^{17} cm^{-2}$)	Σ_N ($10^{17} cm^{-2}$)	Ref.
NO_2^-	1233	1.0×10^{-16}	1.65	0.19	0.19	1
N_2O_x	1300	0.5×10^{-16} [a]	0.73	0.53	1.06	4
		1.0×10^{-16} [b]		0.27	0.54	4
NO_3^-	1337	1.4×10^{-16}	1.58	0.13	0.13	1
NO	1875	4.7×10^{-18}	0.37	0.90	0.90	2
N_2O	2236	7.0×10^{-17}	0.17	0.03	0.06	2
ΔNH_3	1050	1.7×10^{-17} [c]	4.5	3.04	3.04	3
		2.7×10^{-17} [d]		1.92	1.92	5
NH_4^+	1497	7.7×10^{-17} [a,c]	4.7	0.70	0.70	
		4.4×10^{-17} [b,c]		1.53	1.53	
		4.5×10^{-16} [b,d]		0.12	0.12	

Note: The column densities n_x *are the average of four experiments and were calculated by* $n_x(cm^{-2}) = \int_{\nu_1}^{\nu_2} \tau_\nu \, d\nu \; / \; 2A_x$ *(section 2). The factor 2 indicates that the infrared beam passes the sample twice since an IR spectrum was recorded in reflection mode.* ΔNH_3 *was calculated from the decrease of the 1050* cm^{-1} *absorption band of* NH_3. *The values for* $A_{NH_4^+}$ *were calculated using three different combinations of assumptions noted by the combinations a-c, b-c and b-d (see the text for an explanation of the individual assumptions).*

References.- (1) Narayanamurti et al. 1966; (2) Pugh and Rao 1976; (3) d'Hendecourt and Allamandola 1986; (4) see text; (5) unpublished results.

TABLE XI. — *Infrared absorptions and integrated band strengths of ions of astrophysical interest.*

Species	λ (μm)	ν (cm^{-1})	A (cm molecule^{-1})	Reference
NO_2^-	8.11	1233	1.0×10^{-16}	1
NO_3^-	7.48	1337	1.4×10^{-16}	1
NO_3^-	7.19	1390	1.4×10^{-16}	1
NH_4^+	6.86	1458	2.0×10^{-16}	6
$HCOO^-$	6.33	1580	$> 1.0 \times 10^{-16}$ [a]	5
NCS^-	4.87	2052	?	4
CN^-	4.78	2090	1.0×10^{-19}	2
OCN^-	4.62	2165	7.0×10^{-17}	3

a) *Estimated using the assumption* $A(ion) \simeq A(molecule)$

References.- (1) Narayanamurti et al. 1966; (2) Seward and Narayanamurti 1966; (3) Schettino and Hisatsune 1970; (4) Nakamoto 1986; (5) Berckmans et al. 1988; (6) This paper.